

Supported Molten Metal Membranes for Hydrogen Separation

Final Technical Report

Report Period: 9/30/2009 – 9/29/2013

Authors:

Ravindra Datta, Yi Hua Ma, Pei-Shan Yen, Nicholas D. Deveau,
Ilie Fishtik, and Ivan Mardilovich

February 20, 2014

DOE Award No.: DE-FE0001050

Submitting Organization:

Department of Chemical Engineering
Worcester Polytechnic Institute,
Worcester, MA 01609, USA.

Disclaimer

This report was prepared as an account of work sponsored by an agency of the United States Government. Neither the United States Government nor any agency thereof, nor any of their employees, makes any warranty, express or implied, or assumes any legal liability or responsibility for the accuracy, completeness, or usefulness of any information, apparatus, product, or process disclosed, or represents that its use would not infringe privately owned rights. Reference herein to any specific commercial product, process, or service by trade name, trademark, manufacturer, or otherwise does not necessarily constitute or imply its endorsement, recommendation, or favoring by the United States Government or any agency thereof. The views and opinions of authors expressed herein do not necessarily state or reflect those of the United States Government or any agency thereof.

Abstract

We describe here our results on the feasibility of a novel dense metal membrane for hydrogen separation: Supported Molten Metal Membrane, or SMMM.¹ The goal in this work was to develop these new membranes based on supporting thin films of low-melting, non-precious group metals, e.g., tin (Sn), indium (In), gallium (Ga), or their alloys, to provide a flux and selectivity of hydrogen that rivals the conventional but substantially more expensive palladium (Pd) or Pd alloy membranes, which are susceptible to poisoning by the many species in the coal-derived syngas, and further possess inadequate stability and limited operating temperature range. The novelty of the technology presented numerous challenges during the course of this project, however, mainly in the selection of appropriate supports, and in the fabrication of a stable membrane. While the wetting instability of the SMMM remains an issue, we did develop an adequate understanding of the interaction between molten metal films with porous supports that we were able to find appropriate supports. Thus, our preliminary results indicate that the Ga/SiC SMMM at 550 °C has a permeance that is an order of magnitude higher than that of Pd, and exceeds the 2015 DOE target.

To make practical SMM membranes, however, further improving the stability of the molten metal membrane is the next goal. For this, it is important to better understand the change in molten metal surface tension and contact angle as a function of temperature and gas-phase composition. A thermodynamic theory was, thus, developed,² that is not only able to explain this change in the liquid-gas surface tension, but also the change in the solid-liquid surface tension as well as the contact angle. This fundamental understanding has allowed us to determine design characteristics to maintain stability in the face of changing gas composition. These designs are being developed. For further progress, it is also important to understand the nature of solution and permeation process in these molten metal membranes. For this, a comprehensive microkinetic model was developed for hydrogen permeation in dense metal membranes, and tested against data for Pd membrane over a broad range of temperatures.³ It is planned to obtain theoretical and experimental estimates of the parameters to corroborate the model against experimental results for SMMM.

¹ Datta, R., and Yen, P.-S., “Hydrogen Separation Membrane,” Patent Application filed (2013).

² Yen, P.-S., and Datta, R., “Butler-Sugimoto Monomolecular Bilayer Interface Model: The Effect of Oxygen on the Surface Tension of a Liquid Metal and its Wetting of a Ceramic,” submitted to *J. Colloid & Interf. Sci.* (2014).

³ Deveau, N.D., Ma, Y.H., and Datta, R., “Beyond Sieverts’ Law: A Comprehensive Microkinetic Model of Hydrogen Permeation in Dense Metal Membranes,” *J. Memb. Sci.*, **437**, 298-311 (2013).

Table of Contents

1.	Motivation	5
2.	Proposed Membrane Technology and its Rationale	6
2.1	Proposed SMMM Technology	6
2.2	Hypothesis	7
2.3	Selection of Molten Metals.....	9
2.4	Selection of Porous Supports.....	10
2.5	Technology Advantages.....	11
2.6	R&D Challenges.....	11
2.7	R&D Goals.....	12
3.	Permeation Apparatus	12
4.	Evaluation of Different Porous Supports	13
4.1	Porous Metal Supports Found to be Unsuitable	14
4.2	Insights from Thermodynamics of Reactive Wetting	15
4.3	Experimental Evaluation of Suitability of Porous Ceramic Supports	19
4.4	Porous Ceramic Supports Found to be Suitable.....	20
4.4.1	Silicon Carbide.....	20
4.4.2	Graphite.....	21
5.	SMMM Permeance Testing	21
5.1	Hydrogen Permeance of Ga/SiC SMMM	22
6.	Microkinetic Modeling of Hydrogen Permeation in SMMM	27
6.1	Preliminary Theoretical Estimate of Ga SMMM Permeance	28
7.	Resolving the Wetting Instability of SMMM	29
7.1	Theory of Surface Tension and Wetting of Molten Metals	29
7.2	Improving Wettability by Adding a Reactive Component	30
7.3	Membrane Support Sandwich Configuration for SMMM.....	34
7.4	Swagelok Cell SMMM Permeator	35
8.	Conclusions and Future Research	36
8.1	Accomplishments	36
8.2	Further Work	37
8.3	SMMM Fundamental Investigation	37
9.	References	39

1. Motivation

The defining challenge of our time is to find a way to meet the growing need for energy of an increasingly populous and prosperous world without putting the planet in peril. The solution will undoubtedly involve a combination of energy sources. Nonetheless, hydrogen, whether from fossil or renewable resources, could be a common energy vector, as it offers high efficiency and low pollution, especially when used in conjunction with fuel cells. Coal is especially attractive for generating hydrogen, with CO₂ sequestration, because of the vast US reserves. Hydrogen is already produced in huge quantities (Ockwig and Nenoff, 2007), mainly via natural gas to generate syngas, which is then further shifted to hydrogen via the water-gas shift (WGS) reaction. Coal gasification can provide an attractive alternate route to syngas and H₂. However, the H₂ in this comes with other components, i.e., H₂O, CO and CO₂, in addition to contaminants such as H₂S, NH₃, As, Hg, and HCl, etc. Therefore, it must be purified further.

The technologies available for separating H₂ include absorption, membrane separation, pressure-swing adsorption (PSA), and cryogenic distillation (Adhikari and Fernando, 2006; Holladay et al., 2009). The PSA and the cryogenic distillation are the most commonly utilized processes in industry. However, these are energy intensive. It is estimated that 450 trillion Btu/yr could be saved with a 20% improvement in H₂ separation train (DOE, 2005). This is a key reason for seeking alternate H₂ separation technologies, particularly via dense metal membranes. The most promising current membranes involve Pd and its alloys with Ag and Cu, either as thin foils or as thin membranes supported on porous ceramic or metal supports (Paglieri and Way, 2002; Fukai, 2005; Sholl and Ma, 2006; Nenoff et al., 2006; Adhikari and Fernando, 2006; Ockwig and Nenoff, 2007; Yun and Oyama, 2011). However, these membranes still fall short of the desired cost, chemical and mechanical robustness, and durability targets (Table 1). Consequently, the U.S. Department of Energy (DOE) is interested in alternate non-precious group metals (PGM) dense metal membranes that overcome these limitations. The DOE targets for hydrogen membranes are summarized in Table 1 (Driscoll, 2008).

Table 1. The DOE targets for hydrogen separation membranes (Driscoll, 2008).

Membrane Property	Target	
	2010	2015
H ₂ Flux (std m ³ /m ² h)	60	90
H ₂ Feed Pressure, $p_{H_2,feed}$ (psia)	150	150
H ₂ Permeate Pressure, $p_{H_2,perm}$ (psia)	50	50
Operating $\Delta p_{H_2} = p_{H_2,feed} - p_{H_2,perm}$ (psi)	100	100
Operating Temperature, T (°C)	300–600	250–500
Pressure Tolerance, Δp (psi)	400	800–1,000
Sulfur Tolerance (ppm)	20	> 100
CO Tolerance	Yes	Yes
WGS Activity	Yes	Yes
H ₂ Purity (%)	99.5	99.99
Cost (\$/ft ²)	500	< 250
Durability (years)	3	> 5

2. Proposed Membrane Technology and its Rationale

2.1 Proposed SMMM Technology

The overall goal of this project has been to develop and test entirely novel non-PGM supported molten metal membranes (SMMMs) for hydrogen separation that meet the above DOE targets in terms of cost, operating conditions, permeability, selectivity, robustness, and longevity. These membranes are based on low-melting, non-precious group metals (e.g., Sn, In, Ga) and their alloys with transition metals, supported as thin films on an inert porous ceramic or a porous metal support with a ceramic intermetallic diffusion barrier. The goal is to develop hydrogen membranes with good permeability and selectivity that are relatively inexpensive, and are more robust to species such as carbon monoxide, and to poisons such as sulfur, while avoiding challenges related to solid dense membranes, namely, sintering, hydrogen embrittlement, thermal mismatch between the membrane and the support, and formation of pin-holes.

Figure 1 shows a schematic of the proposed supported molten metal membrane. It comprises of a porous ceramic or metal support on which a thin but dense layer of a molten metal or molten metal alloy is deposited (Figure 1). In fact, it is now clear that an oxide/ceramic layer will need to be interposed between the molten metal film and any porous metallic support to avoid diffusion and reaction between the molten metal and the support, as molten metals readily form intermetallic compounds with most metals (Lyon et al., 1950; Westbrook, 1977; Pöttgen, 2006).

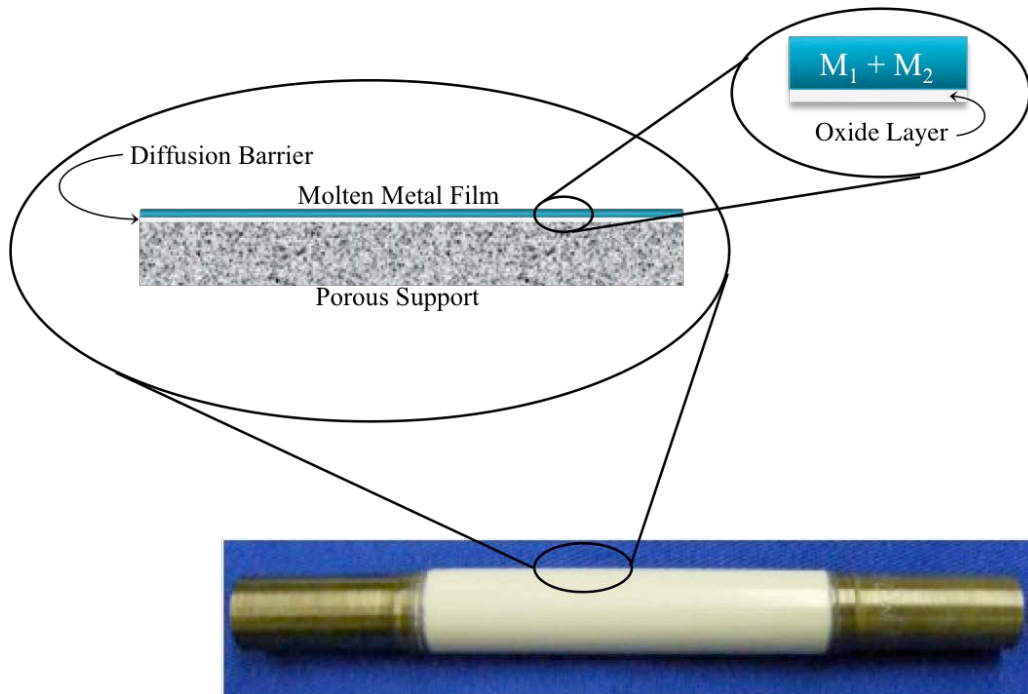


Figure 1. Schematic of supported molten metal membrane (SMMM) on ceramic/PSS support.

The dense molten metal membrane is typically comprised of two components: 1) a low-melting metal (M_1) to provide an open and fluid lattice (Figure 2) desirable for ready dissolution and diffusion of hydrogen atoms, H; and 2) a non-precious group transition, or other catalytic,

metal (M_2), to facilitate dissociation of hydrogen molecules at the membrane surface, in keeping with the accepted mechanism of hydrogen diffusion through a dense metallic membrane, wherein the H_2 molecule first dissociates and adsorbs on the surface (Figure 2), followed by ingress into the lattice, and subsequent diffusion through it, both of which steps are presumably facilitated by lattice defects and vacancies present in a liquid metal film, as shown schematically in Figure 2. The hydrogen atoms then recombine at the downstream surface of the metal into gaseous hydrogen.

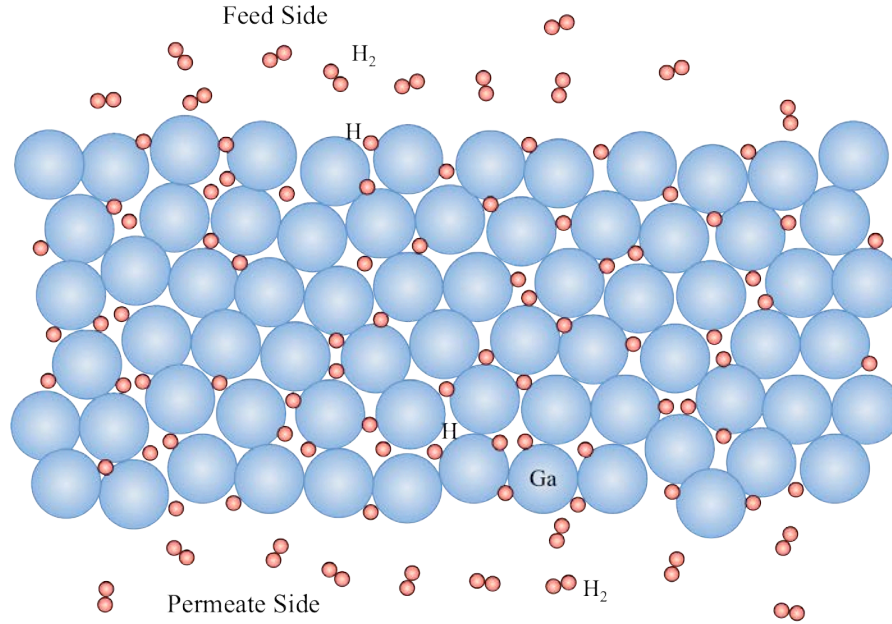


Figure 2. Schematic of molten-metal film structure with interstitial hydrogen.

2.2 Hypothesis

The rationale for the hypothesized higher permeance of SMMM may be understood within the framework of the so-called Sieverts law

$$N_{H_2} = \left(\frac{c_t \chi_{H \cdot M, s} K_S D_H}{2\delta \sqrt{p^\circ}} \right) (p_{H_2, f}^{1/2} - p_{H_2, p}^{1/2}) \equiv P_{H_2} (p_{H_2, f}^{1/2} - p_{H_2, p}^{1/2}) \quad (1)$$

where c_t is the total concentration of the metal atoms, $\chi_{H \cdot M, s}$ is the saturation atomic ratio of adsorbed H per metal atom, K_S is the Sieverts' equilibrium constant for the H_2 solution process, $1/2H_2 + M \rightleftharpoons H \cdot M$, D_H is the interstitial diffusion coefficient of the hydrogen atoms, δ is the membrane thickness, p° is the standard pressure, and p_{H_2} is the hydrogen partial pressure. The second equality in the above defines the permeance of hydrogen, P_{H_2} . In other words, permeance can be increased by increasing solubility K_S and the diffusivity of hydrogen atom, D_H .

A key argument for SMMM is a substantially higher diffusion coefficient for H atoms in liquid metal (Protopapas et al., 1973) as compared to that in a solid metal (Wert and Zener,

1949). Thus, Figure 3 provides a comparison of H diffusion in liquid Ga with that in Pd, showing, not surprisingly, that there is a difference of an order of magnitude between the two.

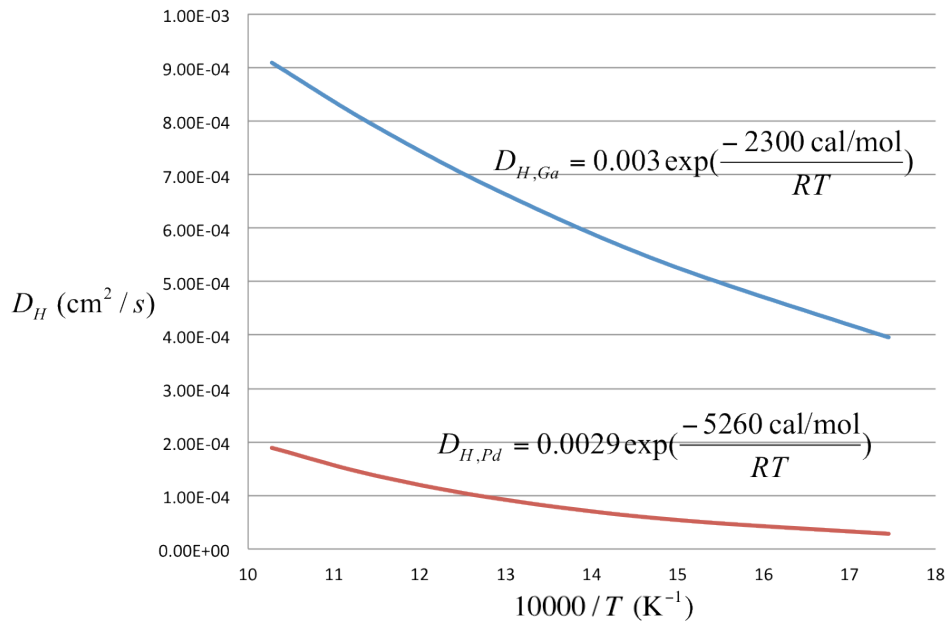


Figure 3. A comparison of H atom diffusion coefficient in Pd and in liquid Ga.

The second argument is that the solubility in a liquid metal is higher, as shown in Figure 4.

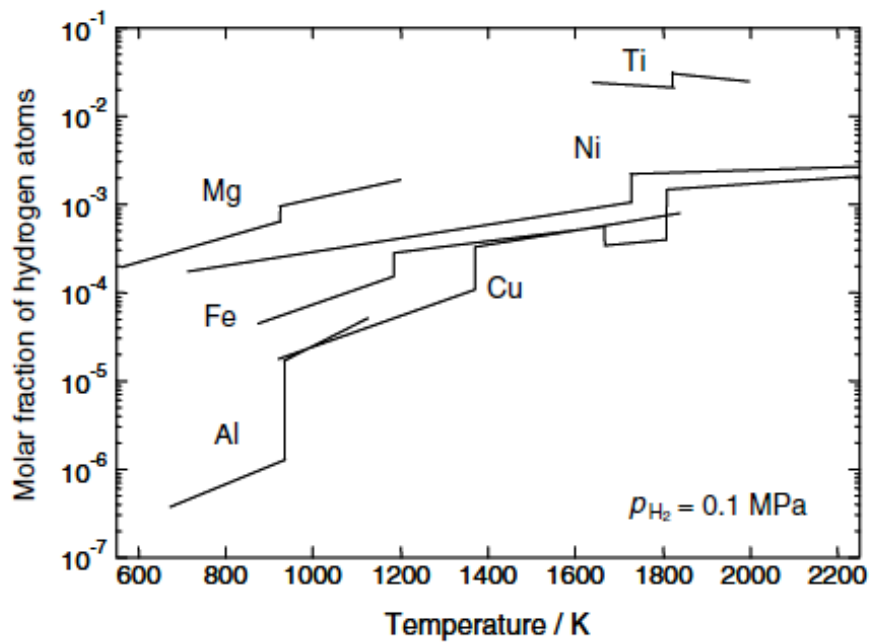


Figure 4. Step change in hydrogen solubility of a metal upon melting (Nakajima, 2007).

As shown in Figure 4 (Nakajima, 2007), the solubility of hydrogen increases with increasing temperature in both solid and liquid forms of a metal, but there is a discontinuous abrupt increase in the solubility at the melting point of a metal.

In short, thus, the hypothesis underlying our proposal for SMMM is that there is a significant increase in both the solubility and diffusivity of hydrogen in a metal, resulting in a higher permeance. There is apparently no precedence for this concept, and thus no guidance in the literature in the selection of metal and support materials, which made for slow going initially in selection of appropriate support materials and in membrane fabrication.

2.3 Selection of Molten Metals

The choice of the low melting metal or eutectic (M_1) was made by perusing the melting points of metals across the period table (Figure 5), with the especially low melting metals of potential interest highlighted.

1	H -259																	He -270	Melting points of the elements /°C
2	Li 181	Be 1278											B 2300	C 3700	N -210	O -218	F -220	Ne -248	
3	Na 98	Mg 649											Al 660	Si 1410	P 44.2	S 119	Cl -101	Ar -189	
4	K 63	Ca 839	Sc 1541	Ti 1660	V 1890	Cr 1857	Mn 1244	Fe 1535	Co 1495	Ni 1455	Cu 1083	Zn 420	Ga 30	Ge 937	As 817	Se 217	Br -7	Kr -157	
5	Rb 39	Sr 769	Y 1522	Zr 1852	Nb 2467	Mo 2610	Tc 2172	Ru 2310	Rh 1966	Pd 1554	Ag 962	Cd 321	In 156	Sn 232	Sb 631	Te 450	I 114	Xe -112	
6	Cs 29	Ba 725	La 921	Hf 2227	Ta 2996	W 3410	Re 3180	Os 2700	Ir 2410	Pt 1772	Au 1064	Hg -39	Tl 304	Pb 328	Bi 271	Po 254	At 304	Rn -71	

Figure 5. Melting points of metals of interest (highlighted).

Of the highlighted metals, those of specific interest to us are Ga, In, Sn, and Bi, and their alloys. In addition to their low cost (Ga is $\sim 1/10^{\text{th}}$ of Pd price, In is $\sim 1/50^{\text{th}}$, Sn is $\sim 1/250^{\text{th}}$, and Bi is $\sim 1/1000^{\text{th}}$ of Pd price), and potentially improved resistance to poisons such as sulfur, these metals are relatively stable possessing a large liquidus range. However, a concern is their potential lack of activity for H_2 dissociation. For this reason, it may be useful to alloy them with a second metal (M_2) to facilitate H_2 dissociation (Figure 2).

The choice of the catalytic metal (M_2) is facilitated by the volcano plot of hydrogen catalytic activity shown in Figure 6, in which exchange current density of the hydrogen electrode reaction is plotted versus the M-H bond strength, indicative of the first steps of the hydrogen permeation process in a dense membrane. As apparent from Figure 6, M_1 candidates (Sn, Ga, Bi) are unlikely to possess sufficient activity for activating H_2 by themselves, at least at low temperatures. Of course, the precious group metals (PGMs), namely, Pt, Pd, Ru, Re, Rh, Os, and Ir, would likely make excellent candidates for M_2 . However, a key intention of this project is to avoid the PGMs.

Consequently, we will focus on other transition metal catalysts that have the potential for activating H_2 (Figure 3), i.e., the group Ni, Co, Cu, Fe, and Ag, as well as some of the early metals on the extreme right of Figure 6, i.e., W, Mo, Nb, and Ta, as alloying with these may move the M-H binding energy of the membrane metal in the appropriate direction closer to the volcano peak. Thus, for example, Ga-Nb, Ga-Ti, or an In-Ni-Nb system may be appropriate. As an additional benefit, as discussed later on, a small amount of some these metals M_2 can also improve wetting between the liquid metal and the porous support.

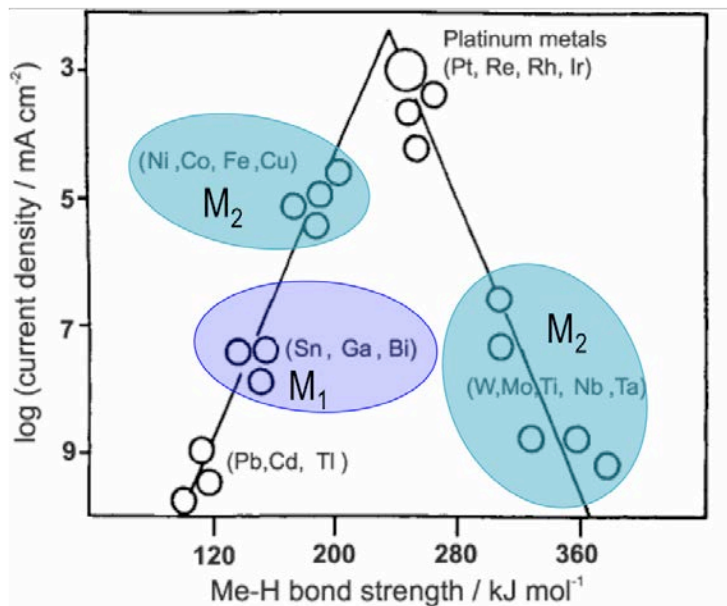


Figure 6. Volcano correlation of hydrogen exchange current density versus M-H binding energy.

The alloying metal can also be used to attain virtually any melting point, as shown by the phase diagram in Figure 7 for the M_1 (Ga) + M_2 (Ag) system. This is important, as the melting point impacts surface tension and viscosity, which are crucial determinants of wetting.

2.4 Selection of Porous Supports

The fabrication of a dense and stable SMM membrane is predicated on the following stringent requirements for an appropriate porous support/diffusion-barrier layer:

1. It should possess chemical inertness, as the molten metals are very reactive, and are likely to infiltrate the support. Thus, we found that most metal supports (except some refractory metals) are not suitable, readily forming alloys and intermetallic compounds (IMCs) with the molten metals at higher temperatures. Many ceramics, on the other hand, are found to possess too much chemical inertness, e.g., Al_2O_3 and ZrO_2 , which are not wetted.
2. The support must possess adequate wettability (contact angle, $\theta < 70^\circ$) for the liquid metal to allow fabrication of a thin, dense, membrane.
3. The support must possess adequate strength to allow compressive sealing, for both disk and tubular geometries, especially at the higher temperatures.

4. The support should possess appropriate pore size and porosity.

This turned out to be a key R&D challenge, as discussed later on.

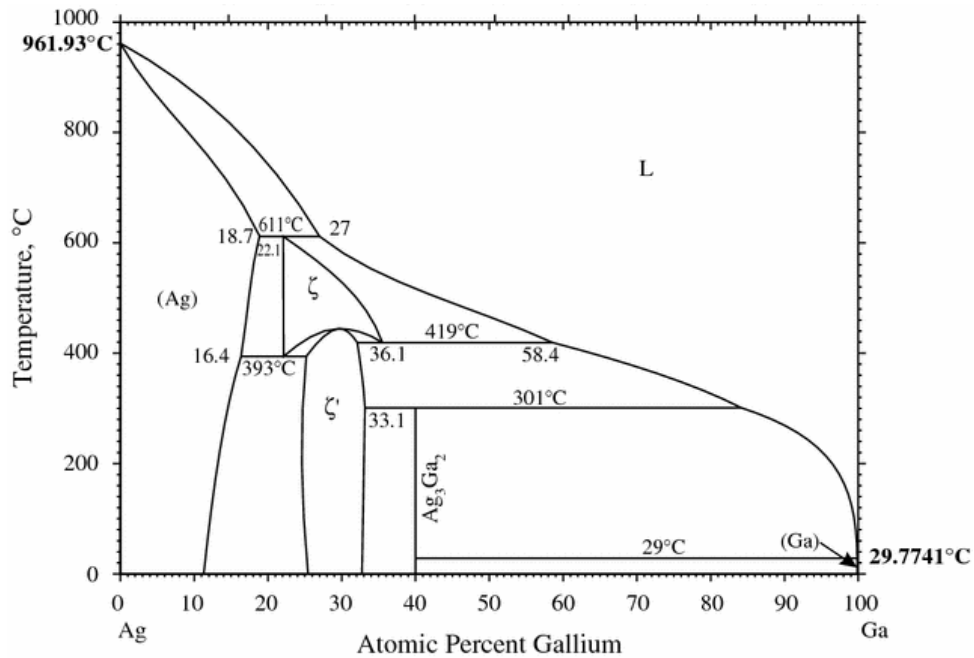


Figure 7. Example of phase diagram of a M_1 (Ga) + M_2 (Ag) system showing that practically any melting point is attainable by selecting the composition (Okamoto, 2008).

2.5 Technology Advantages

- ◆ The SMMM comprises non precious-group metal membranes and, thus, has a substantial cost advantage.
- ◆ Its range of operating temperatures is potentially wider than conventional palladium (Pd)-based membranes.
- ◆ Its permeance is of an order similar to that of Pd or higher.
- ◆ Thermal mismatch issues between metal and support, metal sintering, and hydrogen embrittlement issues are absent.
- ◆ It potentially has better tolerance to sulfur and to other synthesis gas (syngas) components.

2.6 R&D Challenges

- ◆ The SMMM is an entirely novel idea so that there is an absence of prior work in the literature, thereby resulting in a lack of guidance in the selection of metal/support and fabrication procedures.

- ◆ Molten metals were found to be highly reactive and infiltrated all porous metal support at elevated temperatures, rendering them unsuitable, even if pre-oxidized.
- ◆ Most ceramics were found to be too reactive or too inert for good wetting or too fragile to allow compressive sealing at higher temperatures.
- ◆ The wetting characteristics of the molten metal change with the gas environment and with temperature, causing stability issues.

2.7 R&D Goals

The following were the original broad R&D goals of this project:

- ◆ Select molten metals and their supports, develop membrane fabrication protocols, and establish SMMM feasibility.
- ◆ Select and optimize final SMMM candidates and investigate permeability, selectivity, durability, and susceptibility to poisons, as well as microstructural, solubility, and diffusion characteristics.
- ◆ Investigate best SMMM candidates under increasingly realistic conditions.

Due to the challenges described below in fabrication of stable SMMM, progress could not be made on all these fronts. Nonetheless, the initial results obtained are highly encouraging and support the original hypothesis, promising the eventual development of these novel membranes.

3. Permeation Apparatus

A permeation apparatus for testing permeance, selectivity, and durability of tubular or disk SMM membranes for He and H₂, capable of going up to 650 °C, and capable of recording permeation data automatically over an extended period based on Labview[®], was designed and built. A GC was connected directly to the end of the membrane tube side, which allowed a continuous sampling with no air contamination so that it would be possible to accurately analyze the exit gas composition. A schematic of the apparatus is shown in Figure 8.

A few key characteristic features of the permeation apparatus include:

- ◆ A one-inch outer diameter tubular furnace designed for roughly half an inch membranes. The size of the permeator is dictated by the furnace used.
- ◆ Two digital flow meters calibrated for He and H₂.
- ◆ A computer with Labview[®] software for data acquisition.
- ◆ The apparatus was built within a walk-in hood connected to the ventilation system.

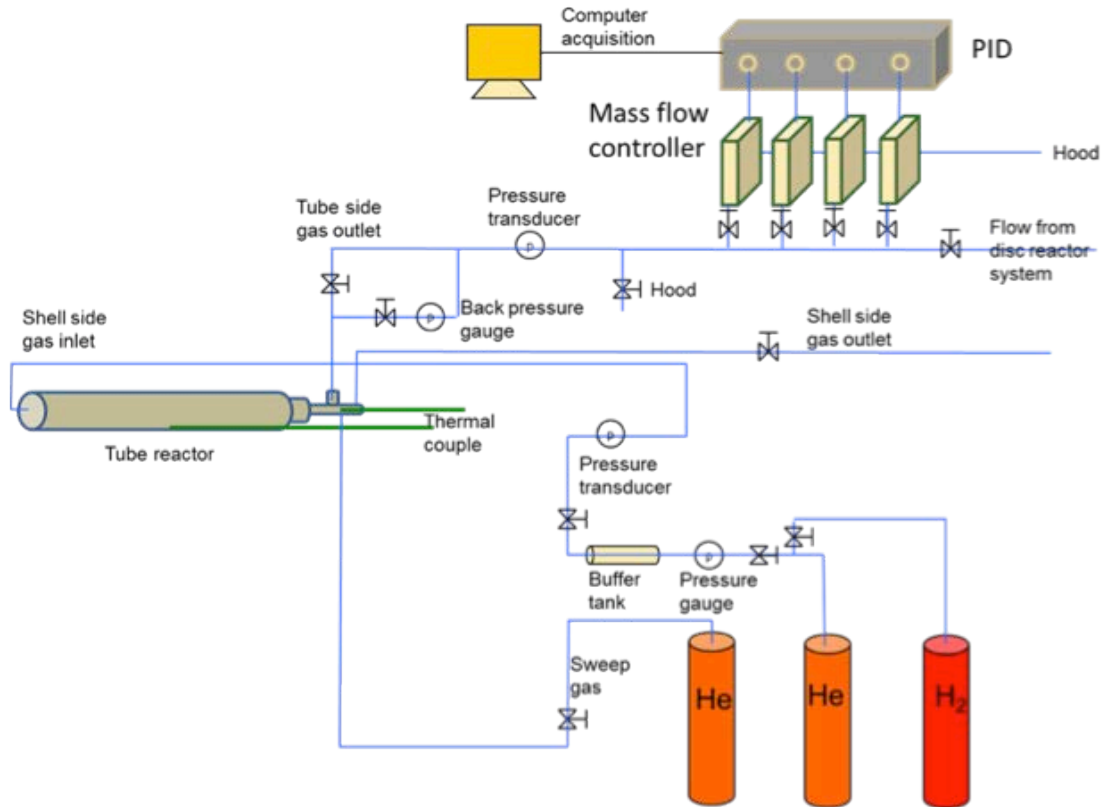


Figure 8. Diagram of hydrogen permeation for ceramic supports test setup.

In addition, a high temperature furnace with controlled gas atmosphere was acquired and used for membrane fabrication.

4. Evaluation of Different Porous Supports

The SMMM is a novel idea, so that there was found to be an absence of any guidance in the literature to help with the selection of metal/support and fabrication procedure. The chief obstacle that emerged, thus, was finding suitable porous supports and intermetallic diffusion barrier layers that are adequately wetted by the molten metals, but are at the same time chemically inert, so that stable SMM membranes may be fabricated. This is a fine balance since some chemical interaction between the liquid metal and the support is necessary for adequate wetting, while too much of it dooms the membrane. Molten metals are, in general, highly reactive.

The various types of porous supports tested for suitability for SMMM included:

- ◆ Porous metal supports (Stainless Steel, Inconel, Nickel, and Titanium),
- ◆ Porous ceramic supports (α -Al₂O₃, Pyrex Glass, Quartz, NiO, ZrO₂, TiO₂, and SiC), and
- ◆ Porous metal support with interdiffusion barrier layer (PSS with ZrO₂ layer) (Figure 1).

In short, thus, based on coupon and tubular support studies, we found that porous metal supports including porous stainless steel (PSS), Ni, Ti, or Inconel, even when oxidized at the usual temperature ($\sim 700\text{ }^{\circ}\text{C}$) to develop an oxide barrier layer, do not provide an effective diffusion barrier that holds up to the liquid metals tested (In, Ga, Sn), because of their high reactivity, leading to the formation of intermetallic compounds. Ceramic supports were more promising. However, some (e.g., Al_2O_3) were found to be too inert to provide good wetting, while others were too reactive, e.g., quartz (Cochran and Foster, 1962), or too fragile for compressive sealing. More details are provided below.

4.1 Porous Metal Supports Found to be Unsuitable

Porous metal supports are standard for the conventional Pd-based membranes (Ayturk et al., 2006). Consequently, these were the first supports that were tested for suitability. Electroless and electroplating were used to deposit molten metals such as Sn-Ni, Sn-Ag, Sn-Cu, Sn-Pd, Sn on the porous Inconel, porous stainless, porous Ni tube. All of the molten membrane deposited on metal support suffered from two major issues. Upon melting, the liquid metal tended to flow, forming droplets on the tube bottoms, and thinning on top, resulting in the development of leaks. Second major issue was found to be the reaction with the formation of intermetallic compounds between the liquid metal and the metal support, confirmed via EDX, so that the membrane was no longer liquid, or even metallic. As shown in Figure 9 (a), the deposited Sn on Inconel was originally shiny silver color which turned into dark gray color after heating up to $600\text{ }^{\circ}\text{C}$, as shown in Figure 9 (b) due to the formation of intermetallic compounds (Pöttgen, 2006). In fact, some of the solid membrane turned into powder under high temperature due to the reaction with hydrogen. Therefore, naked porous metal supports were found to be unsuitable for SMMMs.



Figure 9 (a). A $20\text{ }\mu\text{m}$ dense layer of Sn on the porous Inconel support.



Figure 9 (b). Used Sn/Inconel membrane after permeation experiments up to $600\text{ }^{\circ}\text{C}$.

Thereupon, we tested the suitability of the porous metal supports by first oxidizing them at $\sim 700\text{ }^{\circ}\text{C}$, to develop an oxide intermetallic diffusion barrier, which provides an adequate barrier

against Pd interdiffusion (Ayturk et al., 2006). However, this was ineffective in providing adequate protection against infiltration by liquid metals. However, there were several indications of high H₂ permeance for short bursts when tested before intermetallic reactions destroyed the membranes at high temperatures, which impelled us to continue our search for suitable supports.

4.2 Insights from Thermodynamics of Reactive Wetting

The wetting between a liquid and a solid takes place via the establishment of an interface where bonding occurs. This interaction can be physical, or chemical, i.e., reactive wetting, the propensity for wetting being dependent upon the strength of bonding. Physical wetting involves van der Waals forces (1-10 J/mol) at the interface, while chemical wetting involves chemical reaction (10 – 100 J/mol) between the solid surface and the liquid. For SMMM, due to the high surface tension of the liquid metals, reactive wetting is needed for good wetting.

According to the reaction product interface (RPI) model (Figure 10a), an interfacial product layer is formed by the interfacial reaction, and the final contact angle is determined by the RPI compound, rather than by the parent substrate. However, for a stable membrane, the reaction should be limited to the interface, i.e., a bulk reaction should not occur (Figure 10b).

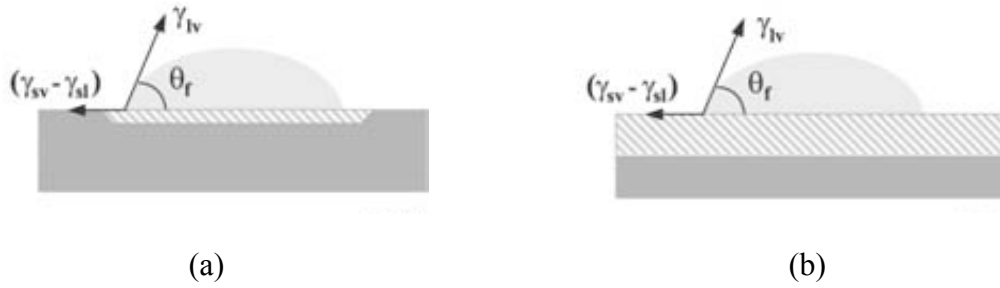


Figure 10. Reactive wetting with the formation of an interfacial layer (a), versus bulk reaction between a liquid and a solid (b).

For reactive wetting, the contact angle

$$\cos\theta = \frac{(\gamma_{sv} - \gamma_{sl}) - \Delta G_{\Sigma}}{\gamma_{lv}} = \cos\theta_0 - \frac{\Delta G_{\Sigma}}{\gamma_{lv}} \quad (2)$$

where ΔG_{Σ} is the Gibbs free energy of the interfacial reaction per unit area, while γ_{lv} is the liquid-vapor, γ_{sv} is the dry solid, γ_{sl} is the wet solid interfacial energy (mJ/m²) or surface tension, and θ_0 is the contact angle in the absence of surface reaction, i.e., for physical wetting.

It is important that the reaction is limited to the interface, i.e., it is not a bulk reaction between the liquid and the support. If it is, the reaction will not be confined to the interface, but the liquid will rather infiltrate the entire solid phase, and components of the solid phase may concomitantly counter-diffuse into the liquid phase. In other words, we are looking for surfaces for which $\Delta G_{\Sigma} < 0$, i.e., the interfacial reaction is favorable, but $\Delta G_r \approx 0$, i.e., the bulk reaction is unfavorable. If $\Delta G_r \ll 0$, bulk reaction would occur between the molten metal and the support

material, as shown schematically in Figure 10b, which would not produce a stable molten metal membrane. Clearly, we are interested in situation represented by 10a rather than that in 10b.

This is clearly a stringent criterion that significantly limits our choices. Fortunately, since surface atoms are more reactive than those in the bulk, since they are missing half their nearest neighbors, i.e., $\Delta G_s < \Delta G_r$, it is possible, in principle, to find a system for which $\Delta G_s < 0$, but $\Delta G_r \approx 0$. Alternately, the RPI layer formed could serve as a diffusion barrier for further interdiffusion between the solid and the liquid phases even though $\Delta G_r < 0$.

As found in our experiments described above, reactive wetting of molten metals proceeds readily on a porous metallic substrate, since $\Delta G_r \ll 0$ for the bulk metallurgical reactions. As a result, upon heating above its melting point, the liquid metal undergoes interdiffusion and reaction to form alloys or intermetallic compounds (IMCs) with the substrate metal. Many of the IMCs have covalent bonds and possess little metallic character or hydrogen permeability. It is possible that metallic character is necessary for good hydrogen permeation if the model of concomitant proton and electron diffusion is accepted for interstitial H transport. Figure 11 shows an example of the post-mortem analysis via energy-dispersive X-ray (EDX or EDS) of the membrane in Figure 9. The EDX cross-section of this membrane is shown in the SEM in Figure 11(a).

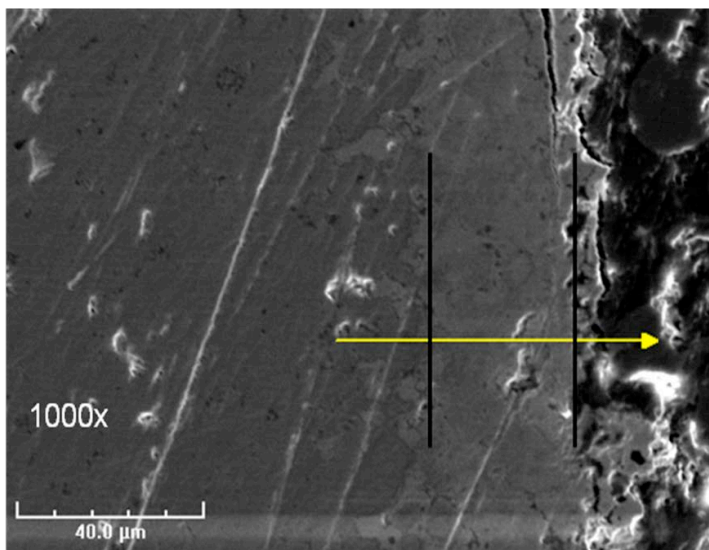


Figure 11(a). SEM of EDX cross-section of Sn/Porous Inconel Membrane.

The deposited Sn is indicated by two straight black lines in Figure 11(a), 11(b), and 11(c). The wide distribution of Pd along the membrane in Figure 11(b) is due to the Pd sputter used in the SEM sample preparation, and a huge peak observed near the outer membrane surface is due to the thin $3.7 \mu\text{m}$ Pd layer used in an effort to improve the hydrogen dissociation rate. Figure 11(c) illustrates the Ni, Cr, Sn and Cu distributions in the membrane. It is clearly seen that extensive inter-diffusion between Ni and Cr present within the Inconel support and the deposited Sn has taken place.

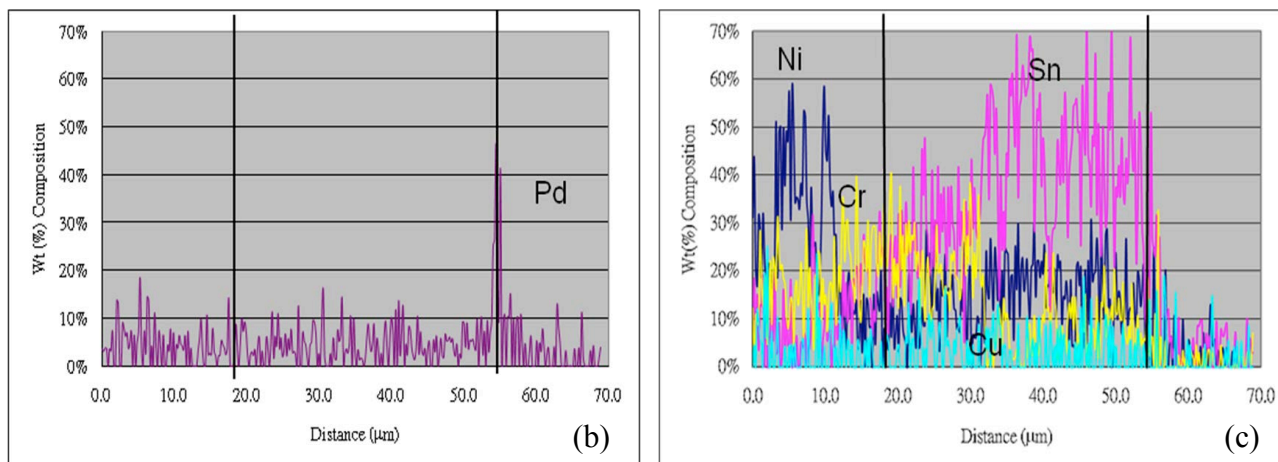


Figure 2(b) and (c). Line scanning result of Sn/Porous Inconel Membrane.

Similar experiments were conducted with a number of porous ceramic supports. Ceramics are tightly bound materials with stable electronic configurations, often ionic, e.g., oxides, and are, thus, largely unreactive toward liquid metals, making them difficult to wet. Covalently bonded ceramics, e.g., diamond, Si_3N_4 , SiC , and BN , also possess strong bonding and stable electronic configurations. Thus, any interaction between a ceramic and a liquid metal is possible only if there is a partial or complete dissociation of its atomic bonds. Fortunately, the surface layer is more reactive, and hence, more amenable to wetting. Wetting is, thus, determined by the affinity of the liquid metal for the anion of a ceramic at its surface ($\Delta G_z < 0$). For instance, wetting of an oxide ceramic would depend upon the affinity of the liquid metal for oxygen.

However, many ceramics (e.g., Al_2O_3 , ZrO_2) were found to be too inert to provide good wetting, while others were too reactive (e.g., quartz). Thus, to narrow down the large number of possibilities based on simply trial-and-error, a thermodynamic investigation of the interaction between the liquid metal and the support material was performed. The calculation is mainly focused on predicting the stability between molten metal and ceramic supports via estimation of the Gibbs free energy change for bulk reaction ΔG_r . If the affinity between the liquid metal and support is large ($\Delta G_r \ll 0$), bulk reaction between them is likely to occur. If on the other hand, $\Delta G_r \gg 0$, the system is inert and non-wettable. Gibbs free energy change in the appropriate range (e.g., $-100 < \Delta G_r < 100$ kJ/mol) would signify affinity needed for wettability without bulk reaction. Coupon tests were subsequently performed to confirm the relationship between stability and wettability.

Possible bulk (or surface) reaction between liquid metal (e.g., Ga) and ceramic support could, thus, be expressed as Eq. (3) for oxide supports and Eq. (4) for nitride supports



Hence, the Gibbs free energy changes for these two reactions are

$$\Delta G_r = y\mu_{O(Ga)} + x\mu_{M(Ga)} - \mu_{M_xO_y} - \mu_{Ga} = y\mu_{O(Ga)} + x\mu_{M(Ga)} - G_{f,M_xO_y}^o \quad (5)$$

$$\Delta G_r = y\mu_{N(Ga)} + x\mu_{M(Ga)} - \mu_{M_xN_y} - \mu_{Ga} = y\mu_{N(Ga)} + x\mu_{M(Ga)} - G_{f,M_xN_y}^o \quad (6)$$

The solubility of metals (M) and oxygen (O) in Ga would be low and may be assumed to follow Henry's law. It is further assumed here that activity is the same as solubility. This assumption has been proven correct as long as the solubility < 2 at% (Yatsenko et al., 2008). The chemical potential of metal in liquid gallium is calculated via

$$\begin{aligned} \mu_{M(Ga)} &= \bar{G}_{M(Ga)} \approx RT \ln a_M = (\Delta S_{Ga} + \Delta S_M)T - (\Delta H_{Ga} + \Delta H_M) \\ \ln a_M &= (\Delta S_{Ga} + \Delta S_M)/R - (\Delta H_{Ga} + \Delta H_M)/RT \end{aligned} \quad (7)$$

The reactivity assessment result of Ga with oxide and nitride supports at 500 °C thus via estimation of Gibbs free energy change of reaction is illustrated in Figure 12. From this, it is noticed that most of the oxide ceramic that have good wetting with Ga are reactive ($\Delta G_r \ll 0$), such as Fe₂O₃/Ga, NiO/Ga, Cr₂O₃/Ga, etc. It means that bulk reaction of Ga with Fe₂O₃, NiO, and Cr₂O₃ takes place at 500 °C. The non-reactive ($\Delta G_r \gg 0$) system such as ZrO₂/Ga, Al₂O₃/Ga, ZrO₂ and Al₂O₃ are inert with Ga at 500 °C, and are thus not wettable. This also matches the experimental wettability assessment of Fe₂O₃/Ga, NiO/Ga and Cr₂O₃/Ga as reactive.

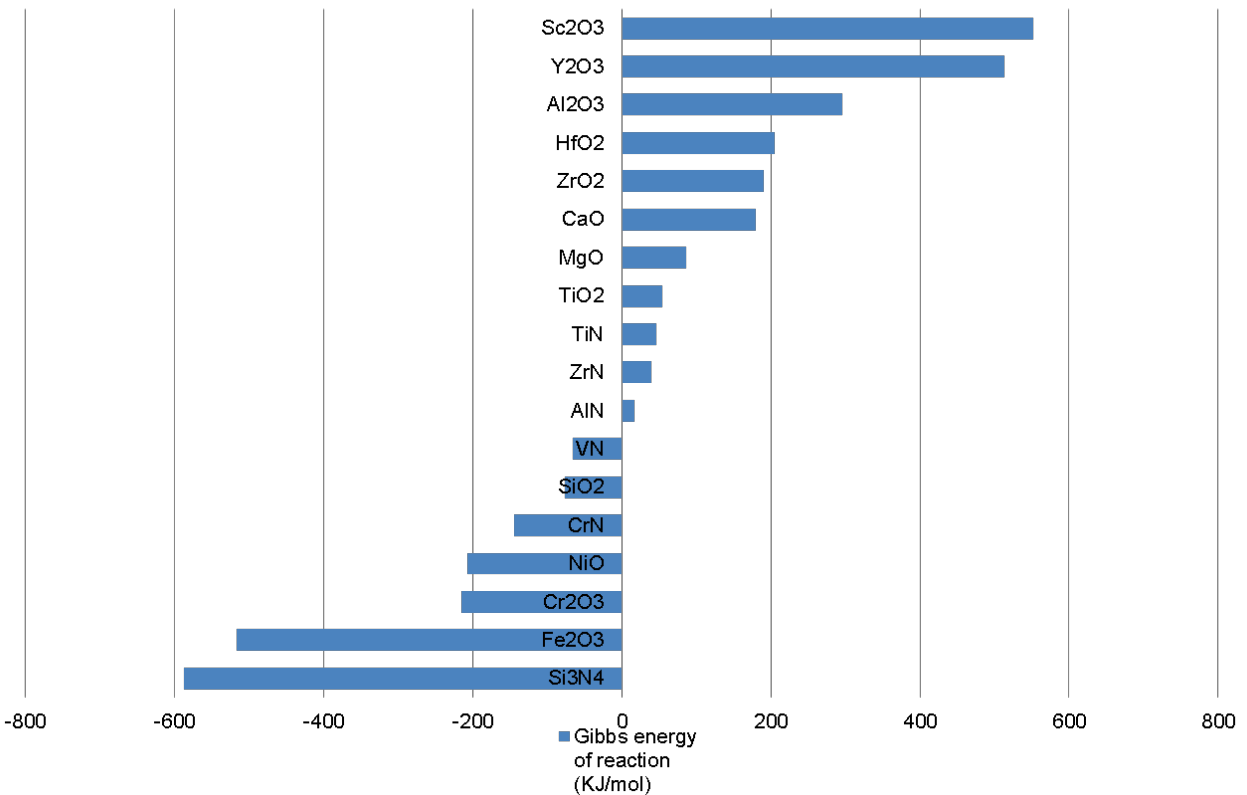


Figure 12. Gibbs free energy change of reaction of oxides and nitrides with Ga at 500 °C.

The actual reactivity of materials in gray area such as, SiO₂, TiO₂, MgO ($-100 < \Delta G_r < 100$ kJ/mol) is unknown, but these may be promising materials with limited reactivity. Based on the above assessment, it is clear that most of the nitrides belong to reactive class and, therefore, may not be suitable candidates as the support for Ga-based membranes. Carbides were, however, excluded in this calculation because of the lack of thermodynamic information of Ga₂C₂ (Samsonov, 1965). The bond Ga-C, like Ga-O, is primarily ionic and is chemically unstable. Hence the wettability and stability of Ga with carbides remains unknown. Though the assessment provides some guidelines in selecting support, the kinetics of the reaction are unknown. A reactive material with very slow kinetics may still be eligible as Ga membrane support, although the operating temperature of around 500 °C likely promotes kinetics. From the thermodynamic assessment above, it was noticed that most of the oxide supports with good wetting with liquid Ga eventually underwent bulk reaction at elevated temperature, including Fe₂O₃, Cr₂O₃, NiO. Further, some of the materials including SiO₂, TiO₂, ZrO₂ maybe debatable in wettability and reactivity calculation.

4.3 Experimental Evaluation of Suitability of Porous Ceramic Supports

In order to confirm the relationship between wettability vs. stability of liquid Ga with supports, thus, various coupons were prepared for testing. The porous supports included SiC, Graphite, Vycor (SiO₂ 96%, B₂O₃ 3%, Al₂O₃, Zr₂O₃, Na₂O less than 1%), ZrO₂, TiO₂, NiO, Al₂O₃ (non-porous), SiO₂ (Quartz). As an example, a quartz frit was found to be unsuitable as it reacted with Ga, as shown in Figure 13.



Figure 13. Quartz/Ga before (a), and after permeability test (b).

Summarizing the conclusions for all the coupon tests, it was found that most of the substrates with proper wetting have poor stability and reacted with Ga over time. Substrates with poor wetting (indicated as X) tend to have good stability (indicated as \checkmark) as shown in Table 2.

Table 2. Experimental result of wettability and stability of various materials at 500 °C.

	TiO ₂	SiO ₂	SiC	NiO	Vycor	Al ₂ O ₃	ZrO ₂	Oxide PSS
Wettability	\checkmark	\checkmark	\checkmark	\checkmark	\checkmark	X	X	\checkmark
Stability	X	X	\checkmark	X	X	\checkmark	\checkmark	X

The lack of chemical reaction on the substrate surface with liquid Ga was one of the reasons for having poor wettability. For a liquid membrane, it is important to find a support with only a slight reaction preferably at the liquid metal and support interface, but not bulk reaction that potentially would destroy the membrane and its ability to permeate H₂.

4.4 Porous Ceramic Supports Found to be Suitable

Based on a thermodynamic and experimental screening, it was determined that SiC is an excellent choice for support. It possesses excellent strength, complete inertness, and adequate wettability to provide dense molten metal membranes.

4.4.1 Silicon Carbide

Porous SiC support was identified as a potentially promising material for fabricating dense molten metal membranes. We thus acquired custom-built porous SiC tubular supports from LiqTech A/S in Denmark (Figure 14 a), with 29% porosity and an average pore size of 10 μm . Membranes of various thickness of room temperature liquid Ga-In alloy could be easily prepared by simply rolling the silicon carbide tubes in the liquid alloy (Figure 14 b). The chemical inertness and stability of SiC supports was established by heating the prepared membranes up to 400 °C in air, and no visible change in the state of liquid alloy was observed. Moreover, the molten metal was found to readily wet the SiC support.

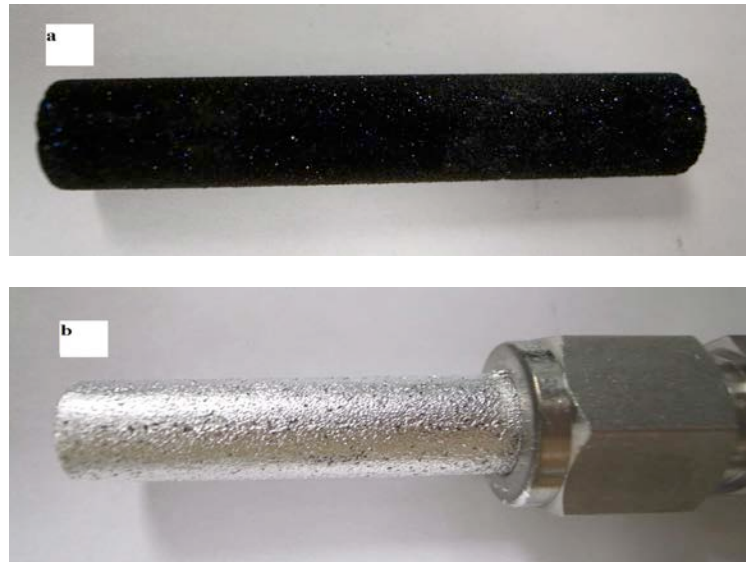


Figure 14. Porous silicon carbide support (a) and Ga-In/SiC membrane (b).

In fact, under vacuum conditions inside the porous tube, drops of liquid alloy could be observed inside the tube walls. In other words, the liquid alloy easily penetrated the porous support. On the other hand, this means that the liquid membrane would not be able to withstand a significant trans-membrane pressure drop. The maximum trans-membrane pressure drop Δp withstood by the liquid membrane of surface tension γ_{lv} and contact angle θ across a support of pore radius $r = 10 \mu\text{m}$ may be calculated using the Young-Laplace equation

$$\Delta p = \frac{2\gamma_{lv} \cos \theta}{r} \quad (8)$$

Thus, for Ga as the molten metal, with $\gamma_{lv} = 708 \text{ mJ/m}^2$ and assuming say $\theta = 45^\circ$, i.e., a reasonably well-wetted support, the maximum trans-membrane pressure drop sustainable is calculated to be 14.5 psi, or only one atm. In order to withstand a higher trans-membrane pressure drop, thus, submicron pore size porous supports are needed. Such porous SiC supports with an assymmetric structure were then acquired from LiqTech. Unfortunately, as discussed later on, the wetting characteristics of molten metal on SiC seemed to change with temperature and gaseous atmosphere under permeation testing, resulting, e.g., in the development of leakage when H_2 is switched to inert He to check selectivity.

4.4.1 Graphite

Finally, another material tested was graphite. Thus, the wettability test results of carbon paper are shown in Figure 15, which is the image of Ga, $\text{Ga}_{62.5}\text{In}_{21.5}\text{Sn}_{16}$ and $\text{Ga}_{75}\text{In}_{25}$ wettability test on carbon paper. Although Ga shows poor wettability with carbon paper, which might be due to the PTEF additive in the carbon paper tested, the other melts showed acceptable wettability with the carbon paper. Similar results were obtained with other forms of graphite, including carbon cloth.



Figure 15. Examples of wettability testing of liquid metals on carbon paper.

5. SMMM Permeance Testing

With the identification of suitable porous supports, efforts were resumed to confirm the high but short-lived hydrogen permeance indicated in earlier experiments with porous metal supports that were destroyed by the reactions resulting in the formation of intermetallic compounds. Thus, SiC was chosen as the support and acquired from LiqTech A/S, Denmark, in disk form, with different pore size. The porous SiC was inserted into a dense Al_2O_3 or SiC tube, as shown in Figure 16 a, and sealed by glass paste. Gallium was melted by heating lamp and deposited on the SiC using vacuum to improve wetting, as shown in Figure 16 b. In early experiments, a dense alumina tube was used, but this arrangement was found to sometimes develop leaks upon heating and cooling during permeance experiments, because of the difference in the coefficient of expansion of SiC and alumina. Consequently, alumina was replaced with SiC dense tube (Figure 16 a). Nonetheless, because of this issue, the glass paste seal also sometimes developed a leak.

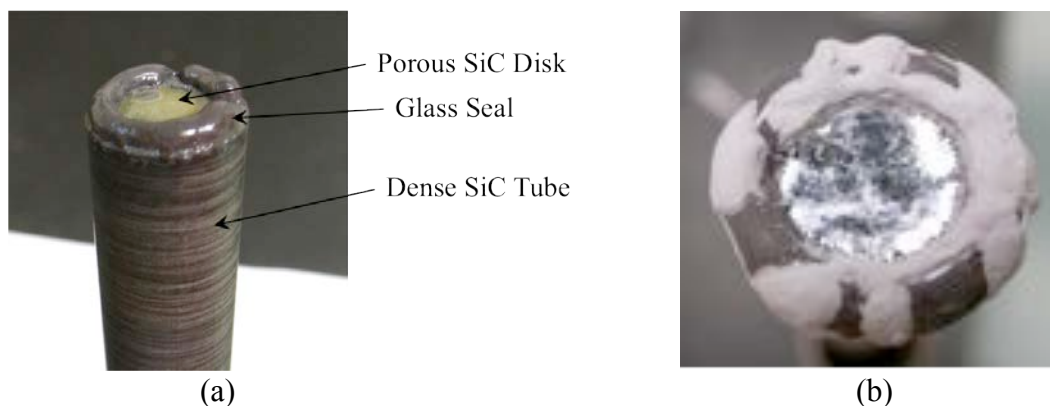


Figure 16. SiC disk permeator sealed via a glass seal in a dense SiC/Al₂O₃ tube (a), with Ga membrane deposited on top (b).

5.1 Hydrogen Permeance of Ga/SiC SMMM

Multiple membranes were prepared and tests were repeated under hydrogen and helium at 500~550 °C and various pressures. For example, the SiC-Ga-7 (423 μm) membrane was tested for about 200 h at temperatures between 450-550°C and pressures 4-13 psi. Hydrogen flux was initially high due to leaks before reaching 500 °C, when *in-situ* glass paste (Figure 16) curing provided a good seal. No flux variation was found thereafter, indicating that molten membrane and sealing were stable for 200 hours. At hour 71, hydrogen flux at 4 psi and 500 °C was still small. At 75 h, the membrane started to show stronger flux at 550 °C, as indicated in Figure 17, once membrane was fully activated. Various pressures were tested using hydrogen and helium to determine the hydrogen flux and selectivity. Several measurements were taken at the same pressure to minimize experimental error. All the measurements were made at least 30 minutes after adjusting the pressure and 1-2 h after gas switching. No helium flux was found at all pressure (4, 6, 8 psi), as seen in Figure 17, so that the membrane was indeed dense.

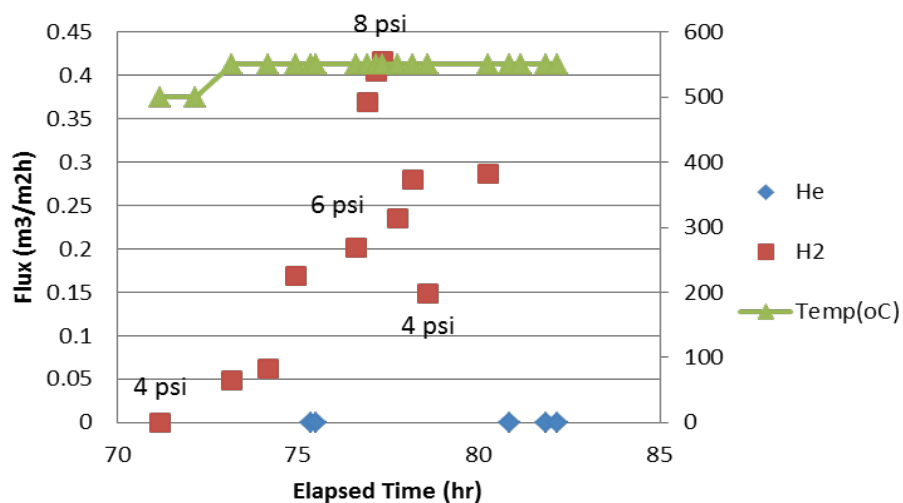


Figure 17. SiC-Ga-7 H₂/He flux at 550°C, 70-85 hour.

Hydrogen permeance of SiC-Ga-7 was determined from the slope in Figure 18, and further compared with SiC-Ga-1 as well as calculated Pd-foil permeance as shown in Figure 18. The two membranes were tested at different temperatures (SiC-Ga-7 at 550 °C, SiC-Ga-1 at 500 °C) and had different initial thicknesses (SiC-Ga-7 423 μm , SiC-Ga-1 678 μm). The calculated Pd permeance for membrane thickness 423 μm at 550 °C was $1.52 \text{ m}^3/\text{m}^2\text{atm}^{0.5}$ and Pd permeance for 678 μm at 500 °C was $0.82 \text{ m}^3/\text{m}^2\text{atm}^{0.5}$. Ga permeance was calculated by fitting trend line in Figure 18. In both cases R^2 was higher than 0.99. The measured Ga hydrogen permeance at different thickness and temperatures thus showed similar hydrogen permeance to Pd membrane.

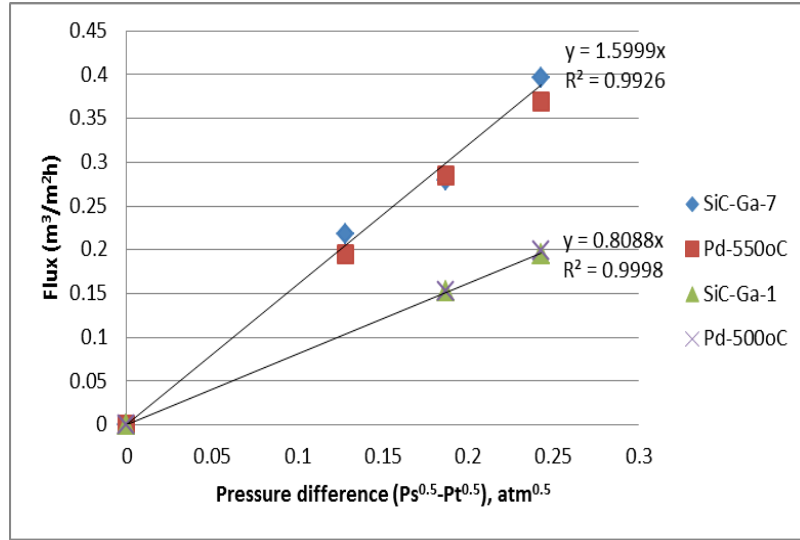


Figure 18. Ga hydrogen flux and calculated Pd hydrogen flux-case 1 (based on initial membrane thickness).

The initial thickness of membranes above was calculated using the plated Ga weight before experiment. It was found, however, that after the experiment the weight of Ga had decreased. Thus, the final thickness for SiC-Ga-7 was 254 μm . For SiC-Ga-1, the final membrane thickness after experiment was unknown; however, it was estimated as between 478~678 μm . The reason for this decline in thickness is not yet entirely clear. It is conceivable that this is simply from Ga physical volatilization. The vapor pressure calculated for Ga is exceeding low, however, i.e., $6 \times 10^{-7} \text{ Pa}$ at 550 °C. Therefore, it seems unlikely that physical vaporization is the main cause of Ga membrane thinning. An alternate plausible mechanism for membrane thinning might be that GaH_2 is formed at the higher temperatures under the hydrogen atmosphere, which is more volatile. This needs to be confirmed further, however, and if indeed determined as a cause of membrane thinning, then mitigation strategies would need to be developed, e.g., via alloying.

Since the thickness had changed, Ga permeance was also compared with Pd for the lower membrane thickness, as shown in Figure 19. Calculated Pd permeance at 550 °C, 254 μm thus is $2.54 \text{ m}^3/\text{m}^2\text{atm}^{0.5}$, and Pd permeance at 500 °C, 478 μm was $1.16 \text{ m}^3/\text{m}^2\text{atm}^{0.5}$. In this case, both of the Ga hydrogen permeances were about 65% of the calculated Pd hydrogen permeance.

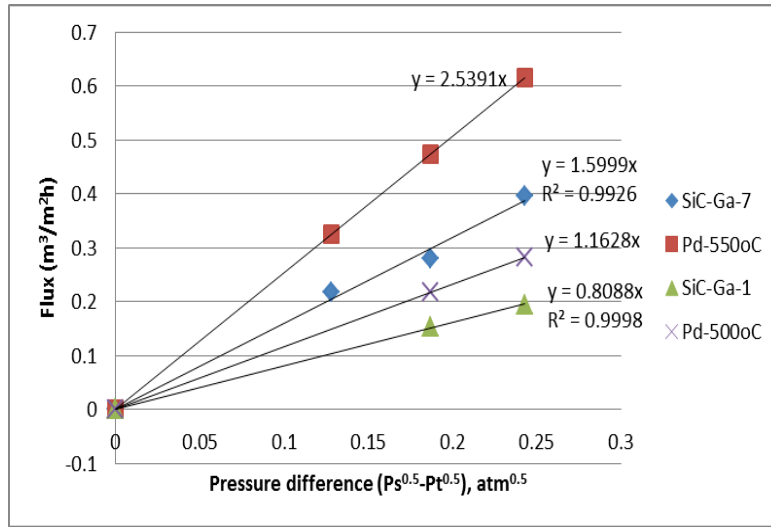


Figure 19. Ga hydrogen flux and calculated Pd hydrogen flux-case 2 (based on final membrane thickness).

Though, the possibility that part of the hydrogen flux was contributed by leakage cannot be ruled out, however, it should be relatively small because no helium flux was found in both cases described above. Thus, it might be concluded that Ga hydrogen permeance of SiC-Ga-1 and SiC-Ga-7 is at least 65% of the hydrogen permeance for pure Pd membrane of the same thickness at 500-550 °C. In other words, permeance of Ga is apparently of the same order as Pd.

Membrane SiC-Ga-8 with thickness of 269 μm was next prepared for the testing, the results of which are shown in Figure 20.

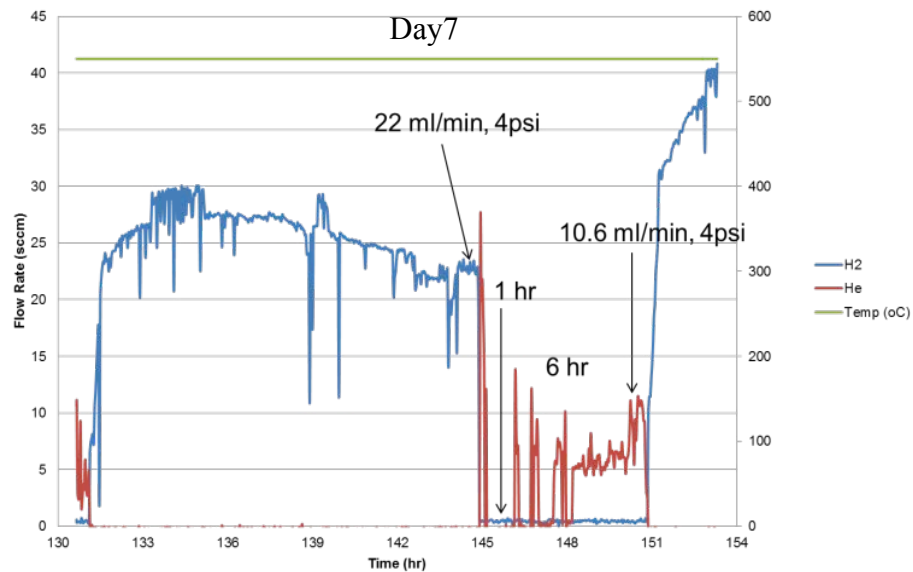


Figure 20. SiC-Ga-8 H₂/He flux on Day 7.

Despite being thinner than previous membrane, it took over 100 hours to activate this membrane. The processes that constitute membrane activation are not yet clear, but it is evident from the lack of any flux in the first 100 h that the membrane made is dense. Upon activation, experiments with hydrogen on Day 7 shown in Figure 20 show that the flux of H₂ is significant and relatively stable for roughly 12 h at 550 °C. The feed gas was thereupon switched to He to make sure that there was still no leakage. The absence of He leakage was confirmed as no flow was observed for a period of one hour. However, then it started to oscillate, eventually increasing to 10.6 ml/min after 3 h in helium. It was then realized that while the membrane was likely dense in hydrogen, it was the switch to He that caused membrane instability. In other words, it appeared that the surface tension and, consequently, wetting behavior was dependent on the gas-phase environment. After switching from helium back to hydrogen, the surface tension and wetting apparently changed again and perhaps some of the local leakage was removed.

Since membrane was not stable under helium atmosphere for more than an hour, it was still needed to check membrane selectivity. Therefore, the usage of helium was controlled to the minimum. On days 9~11, thus, after hydrogen flow rate measurements were performed, helium was used for only 1 h as shown in Figure 21 (a), (b), and (c).

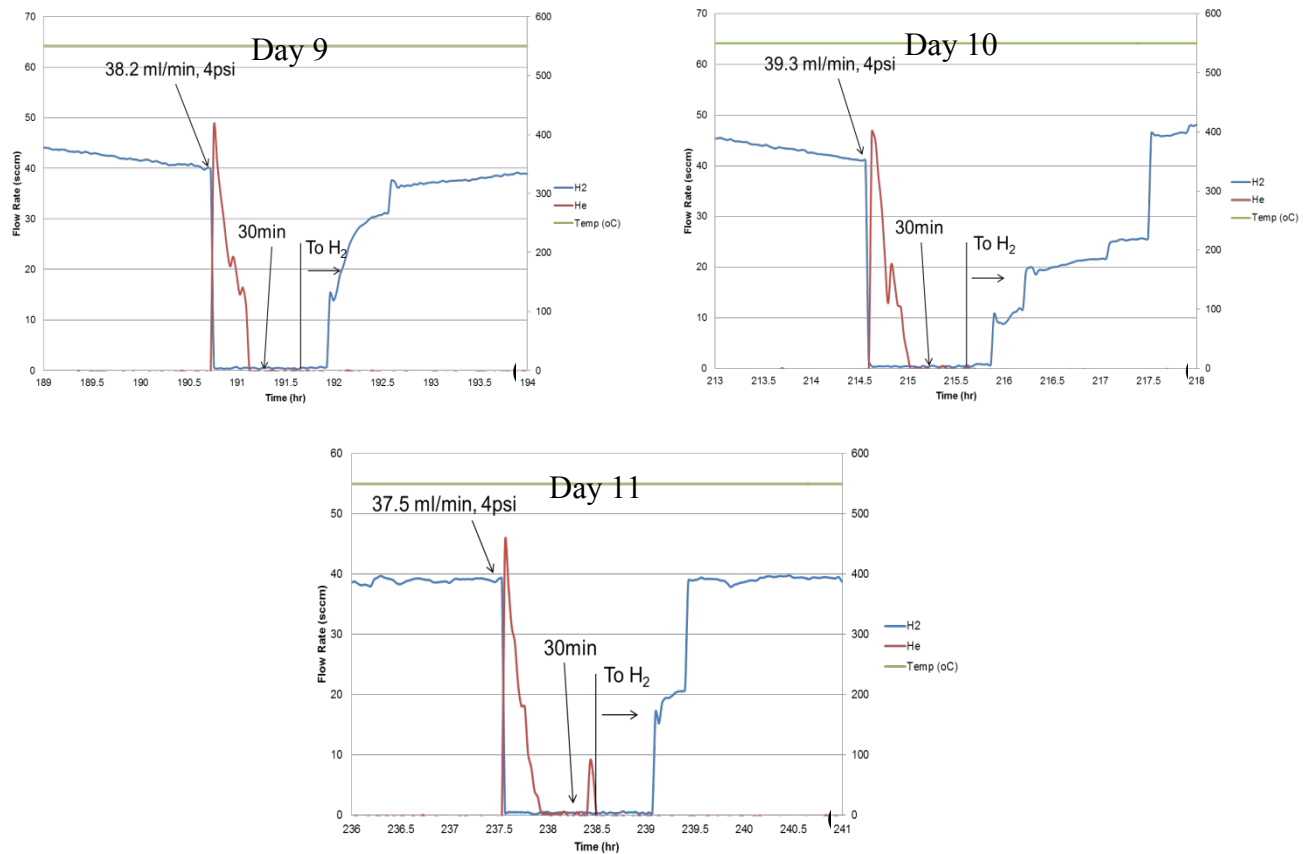


Figure 21. SiC-Ga-8 H₂/He flux at (a) Day 9, (b) Day 10, and (c) Day 11.

The hydrogen flow rate was very similar on these days, ranging from 37.5~39.3 ml/min (equals to 48.15~50.46 m³/m²h, 376.45~394 m³/m²h atm^{0.5}) at 4 psi, as seen in Figure 21, which

is half of the DOE 2015 goal (Table 1) even at a much smaller pressure drop. After switching to He, some gas flow rate was still observed for about 30 minutes, presumably due to the desorption of the H₂ absorbed within the molten metal membrane. After about 30 minutes in helium, all the hydrogen remaining in the cell and membrane was gone and helium flow dropped to zero, which lasted for 30 minutes, before switching back to hydrogen. Upon switching gas back to hydrogen, the flow did not commence immediately, but rather roughly after 20~30 minutes of hydrogen flow. This proved conclusively that there was no leakage from sealing and any small pinholes in the membrane. Further, the transient in flow upon switching between H₂ and He could conceivably provide a good estimate of the hydrogen solubility in Ga at 550 °C.

Hence, it was assumed that membrane was dense from Day 9-10, and also dense on Day 6-7 before helium damaged the membrane. The final thickness of SiC-Ga-8 membrane was unknown; however, the calculated hydrogen permeance of 376 m³/m²h atm^{0.5} is equivalent to permeance of a Pd membrane of a thickness of only 1.7 μm, suggesting that Ga could potentially have a higher hydrogen permeance than Pd, perhaps as much as an order of magnitude or more higher. Further, this is higher than the DOE target for 2015.

The activation energy for the SiC-Ga-8 membrane was determined by changing temperature at fixed pressure drop. In order to ensure no leakage, only permeance at low pressure was measured at temperatures higher than 500 °C. The activation energy at 3 psi and temperatures between 520-565°C is determined as shown in Figure 22, and found to be 16.2 kJ/mol.

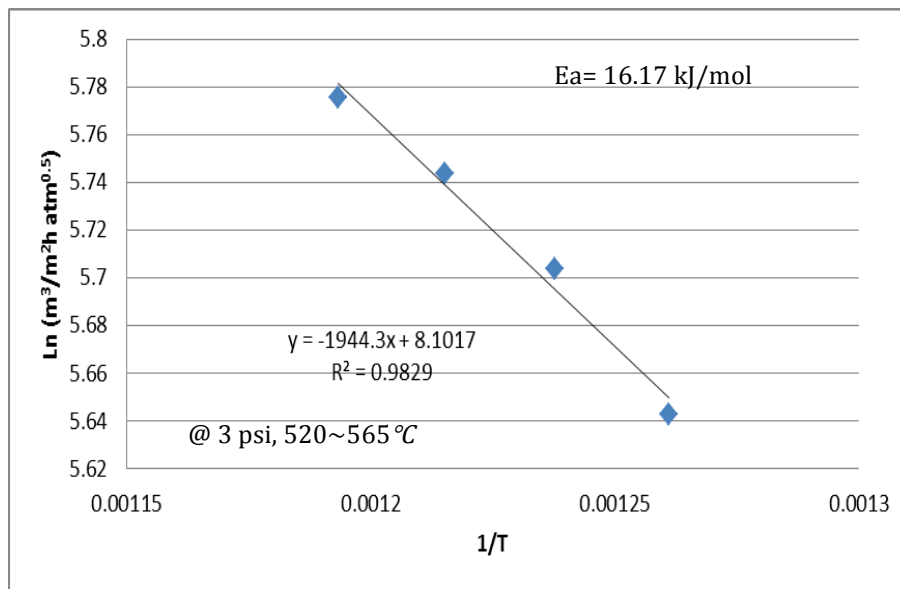


Figure 22. Activation energy of membrane SiC-Ga-8.

From the experimental tests described above, it is concluded that Ga membrane may well have a hydrogen permeance similar to, or up to an order of magnitude higher than, Pd. However, this membrane was not stable because of the change in the surface tension and wetting of Ga with the change in gas atmosphere between H₂ and He. It is, thus, important to understand this

behavior (Yen and Datta, 2014) to be able to overcome it. Only then can one make irrefutable assertions regarding the superiority of these membranes, as well as their practical import.

6. Modeling of Hydrogen Permeation in SMMM

While the exact permeance of the Ga/SiC SMMM as compared to that of Pd reported above may be as yet debatable, because of the physical instability of the membrane as a result of the change of the surface tension and wetting behavior of liquid metals, it is clear that Ga possesses significant hydrogen permeability and, thus, may well have practical significance in the future. Clearly, then it would be prudent to look into both the reasons for the membrane instability owing to wettability changes, as well as into the detailed mechanism and characterization of hydrogen permeation in SMMM. We have made theoretical progress in both these aspects (Deveau et al., 2013; Yen and Datta, 2014), and plan to do some further work as described later to experimentally determine the needed parameters.

The mechanism of hydrogen permeation in a liquid metal is likely similar to that in a solid metal membrane such as Pd, as shown schematically in Figure 23.

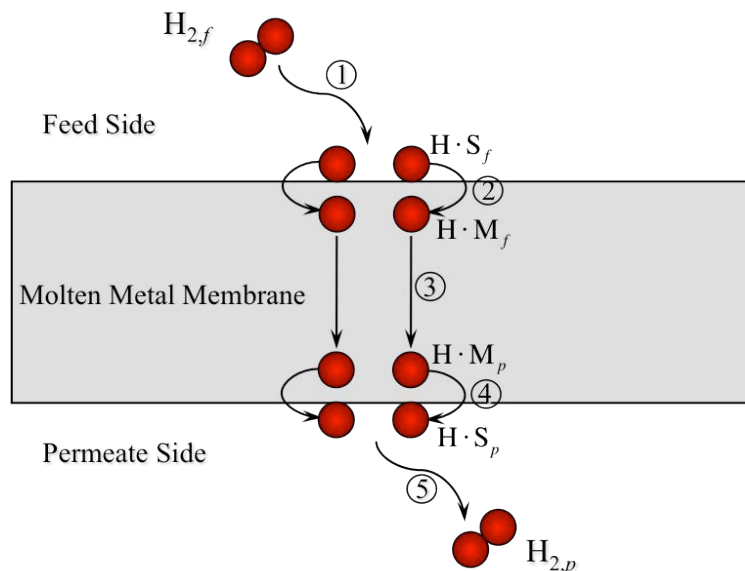


Figure 23. A schematic of hydrogen permeation through SMMM involving sequential steps of surface dissociative adsorption, subsurface penetration, bulk metal diffusion, egress to surface, and reassociation of H atoms.

Since it is not clear at this time which of these steps may be rate-limiting, if any, for hydrogen permeation in a given SMMM, we have developed a comprehensive microkinetic model of permeation in dense metal membranes (Deveau et al., 2013), which will be utilized once the parameters, for instance, for Ga are available.

Nonetheless, the key parameters that determine the permeance are solubility and diffusivity of H atoms in a dense metal membrane. These are expected to be higher in a liquid metal than the corresponding values in a solid crystalline metal, simply because of the disordered liquid structure and larger interatomic distance (Figure 2). Thus a step increase in solubility of hydrogen is observed typically in a metal at its melting point (Figure 4). However, because the

hydrogen dissociation activity of these metals (step 1, Figure 23) is expected to be smaller than Pd, the resulting hydrogen solubility would typically be lower.

On the other hand, the hydrogen diffusion coefficient is expected to be higher, as shown in Figure 3. Consequently, the overall permeance may be expected to be of the same order as Pd. This appears indeed to be borne out experimentally, as discussed above.

6.1 Preliminary Theoretical Estimate of Ga SMMM Permeance

Although the parameters for estimating the Ga permeance from the detailed microkinetic model are not yet available, here we make a preliminary effort to confirm the experimental indication of a high permeance based on assuming Sieverts' law, and using early estimates of solubility and diffusivity of H₂ in Ga. Thus, from Eq. (1), the permeance of hydrogen (Deveau et al., 2013)

$$P_{H_2} = \frac{c_t \chi_{H-M,S} K_S D_H}{2\delta \sqrt{p^o}} \quad (9)$$

based on the Sieverts' law solubility of hydrogen

$$\chi_{H-M} = (\chi_{H-M,S} K_S) \sqrt{p_{H_2}} \quad (10)$$

along with an early estimate of the diffusion coefficient of Ga (Mazayev and Prokofiev, 1994), as shown in Figure 3, i.e.,

$$D_H = D_{H,0} \exp\left(-\frac{E_\mu}{RT}\right) \quad (11)$$

where $D_{H,0} = 3 \times 10^{-7}$ m²/s, and the activation energy $E_\mu = 2,300$ cal/mol. Further, the concentration of metal atoms

$$c_t = \frac{\rho_M}{AW_M} \quad (12)$$

The density of Ga at room temperature is $\rho_M = 6085.2$ kg/m³, while that at 550 ° C, $\rho_M = 5704.7$ kg/m³, (Chentsov et al., 2011), the atomic weight, $AW_M = 69.7$, so that $c_t = \rho_M / AW_M = 5.7047/69.7 = 0.08185$ mol/cm³. The membrane thickness, $\delta = 269$ μm at room temperature calculated from membrane mass, $m_M = 0.1287$ g, and membrane area, $A_M = 0.785$ cm², while that at 550 ° C, $\delta = 287$ μm. Thus, all of the terms in Eq. (13) are known except for the hydrogen solubility χ_{H-M} , which is determined as follows.

When H₂ feed is switched to He, the H₂ that is already in the upstream tubing and dissolved within the membrane continues to evolve, as seen in Figures 20 and 21, before the flux becomes zero as expected for He in a dense membrane. This quantity is estimated as follows: 523.3 scc on Day 7, 490.6 scc on Day 8, and 409.7 scc on Day 9. As a conservative estimate, let us assume this to be the least amount, i.e., 409.7 scc. From this must be subtracted H₂ that is already in the tubing when the switch in feed is made, the volume of which is estimated as 230 cc. Although this must be corrected for temperature (some of it at room temperature, and some at higher) and

pressure (4 psig), as a rough estimate, we simply assume this as 230 scc H₂. Therefore, hydrogen solubility in Ga membrane is 409.7 – 230 = 179.7 sccm, or $n_{H_2} = 8 \times 10^{-3}$ mol H₂. On the other hand, the number of moles of Ga in the membrane, $n_M = m_M / AW_M = 0.1287 / 69.7 = 1.847 \times 10^{-3}$ mol. Thus, the hydrogen solubility at 550 °C, $\chi_{H-M} = 2n_{H_2} / n_M = 2 \times 8 \times 10^{-3} / 1.85 \times 10^{-3} = 8.7$. Using this in Eq. (10), this provides roughly 8 H atoms per Ga atom at atmospheric pressure of H₂, which is a very high solubility, likely explained by the significant vacancies present in a liquid metal (Figure 2).

Finally, using the hydrogen diffusivity in Ga at 550 °C given by Eq. (11), $D_H = 7.3 \times 10^{-8}$ m²/s, along with the other parameters above, this provides from Eq. (9) a permeance of

$$P_{H_2} = 6.3 \times 10^3 \frac{\text{std m}^3}{\text{m}^2 \text{ h } \sqrt{\text{atm}}} \quad (13)$$

Using this in Eq. (1), the flux under the experimental conditions of $p_{H_2,f} = 4$ psig, or 1.272 atm. and $p_{H_2,p} = 1$ atm

$$\begin{aligned} N_{H_2} &= P_{H_2} \left(\sqrt{p_{H_2,f}} - \sqrt{p_{H_2,p}} \right) \\ &= 6.3 \times 10^3 \left(\sqrt{1.272} - \sqrt{1} \right) = 800 \frac{\text{std m}^3}{\text{m}^2 \text{ h}} \end{aligned} \quad (14)$$

The actual flux, $N_{H_2} = 50 \frac{\text{std m}^3}{\text{m}^2 \text{ h}}$ flux, i.e., an order of magnitude lower. Nonetheless, the experimental permeance is substantially higher than the DOE 2015 target.

7. Resolving the Wetting Instability of SMMM

It is, thus, clear that permeance of the SMMM can readily exceed the DOE 2015 targets. However, to make these membranes practical, the wetting instability of these membranes with changing gas atmosphere needs to be first addressed. Therefore, we have embarked on a theoretical understanding of the effect of the gas composition on the surface tension and wetting of molten metal, as briefly described below, and in more detail in Yen and Datta (2014). Further, we are developing a novel design for these molten metal membranes of the sandwich configuration, which would obviate the issue of their wetting instability.

7.1 Theory of Surface Tension and Wetting of Molten Metals

It is clear from experiments that the wetting characteristics of the SMMM change when H₂ is switched to He or vice versa. In fact, there is a considerable discussion in the literature of the effect of oxygen on liquid-gas surface tension of molten metals, which has been well-investigated experimentally and modeled theoretically via the Szyszkowski equation

$$\sigma_{LG} = \sigma_{LG}^o - \Gamma^o RT \ln(1 + Ka_O) \quad (15)$$

where σ_{LG} is the liquid-gas surface tension, σ_{LG}^o is the surface tension in the absence of oxygen, Γ^o is the saturated oxygen adsorption concentration at the liquid surface (mol/m²), K is the

equilibrium constant for oxygen adsorption, and a_o is the activity of oxygen in the liquid metal. This is derivable from the Butler molecular monolayer interface model. However, there is no corresponding model describing the experimentally observed profound effect of oxygen partial pressure on solid-liquid surface tension as well as on contact angle of molten metals on ceramic substrates.

Consequently, we utilized the Butler-Sugimoto thermodynamic approach based on a monomolecular bilayer interface model to investigate the effect of oxygen partial pressure on liquid-gas and solid-liquid surface tension of molten Cu/Al₂O₃ and molten Ag/Al₂O₃ systems. It was found that, in general, the surface tension between phases α and β comprised of matrix components A and B, respectively

$$\sigma_{\alpha\beta} = \sigma_{\alpha\beta}^o - \Gamma_A^{\alpha,o} RT \ln \frac{a_A^\alpha}{a_A^{\Sigma\alpha}} - \Gamma_B^{\beta,o} RT \ln \frac{a_B^\beta}{a_B^{\Sigma\beta}} \quad (16)$$

where a_A^α is the bulk phase activity of A while $a_A^{\Sigma\alpha}$ is that in the surface monolayer.

Further, with the assumption of Langmuir adsorption of a solute species on the surface, this reduces to

$$\sigma_{\alpha\beta} = \sigma_{\alpha\beta}^o - \Gamma_A^{\alpha,o} RT \ln(1 + K_i^{\Sigma\alpha} a_i^\alpha) - \Gamma_B^{\beta,o} RT \ln(1 + K_j^{\Sigma\beta} a_j^\beta) \quad (16)$$

It was, thus, found that both liquid-gas and solid-liquid surface tension are a strong function of oxygen activity in the melt, which, in turn, depends on gas-phase oxygen partial pressure, in conformity with experiments. The change of solid-liquid surface tension and wetting is also greatly affected by the change of in liquid-gas surface tension.

This improved understanding would be of immense help in understanding the wetting instability in SMMM, and how it might be addressed.

7.2 Improving Wettability by Adding a Reactive Component

As indicated above (Eq. 16), both gas-liquid and solid-liquid surface tension and, hence, wetting can change dramatically by the addition of a small amount of another substance. This applies not just to gaseous components but also to trace amounts of other metals. Thus, wetting might be enhanced by alloying the liquid metal with small amounts of another metal, e.g., Ti. Thus, an interfacial filler metal, having a higher affinity, e.g., for oxygen at the ceramic surface, might enhance wetting of these metals. Many refractory metals such as Ti, Nb, Sc, V, Zr, Cr, W, and Mo (and Li), possess good reactivity, and can completely spread onto the most common structural ceramics, i.e., Al₂O₃, ZrO₂, TiO₂, SiO₂ and MgO, and are, thus, good interfacial fillers. Incidentally, these metals might also help in improving the hydrogen dissociation ability of the membrane, i.e., serving effectively as catalyst metal M₂. Thus, addition of small amounts of these reactive elements could substantially improve the wetting of ceramic substrates by diffusion and interfacial reactions of these species to form a RPI.

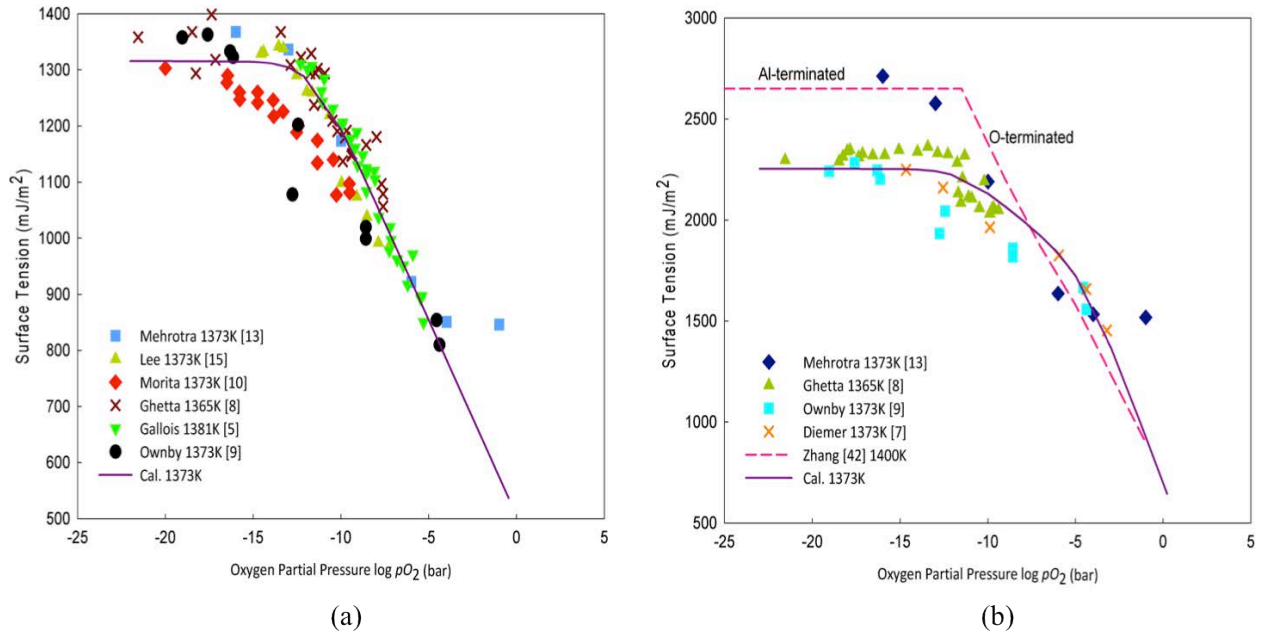


Figure 24. Comparison of our model with experimental results from the literature on the effect of the partial pressures of oxygen on the liquid-gas (a) and solid-liquid (b) surface tension of Cu at 1373 K for the molten Cu/Al₂O₃ system.

For many liquid metals, the liquid-gas surface tension is too high (Iida and Guthrie, 1988), so that physical wetting of many solid surfaces by molten metals is difficult. Wettability is influenced by physical factors such as pore and support geometry, and chemical factors such as chemical bond between the liquid metal and the solid support at the interface, which could be affected by working temperature, functional groups. To promote a reaction, and hence wetting, between molten metal and a ceramic surface, including oxygen free substrate such as TiC, SiC, and TiN, has been investigated at considerable length in the field of metal-ceramic brazing (do Nascimento et al., 2003). By forming strong chemical bonds such as metallic bonds or covalent bonds (like Si/SiC, Al/TiN system) can directly influence contact angle and work of adhesion by adsorption to the liquid/solid or liquid/gas interface.

For instance, the contact angle of SiC/Ga at 800 °C is about 118°, and σ_{LG} is 660 mJ/m² (Asthana, 1994; Eustathopoulos et al., 1999). Having moderate wetting (< 90°) at 500 °C is our goal. Although, there is no direct work reported in literature on the SiC/Ga wetting improvement, similar research has been done for sapphire, quartz, and graphite with Ga (Naidich and Chuvashov, 1983). The contact angle between sapphire, quartz, and graphite with Ga decreases with increasing temperature. By adding small percentages of refractory metals such as Ti, Cr, V into Ga the wettability with aforementioned materials at 900 °C shows great wetting improvement (Naidich and Chuvashov, 1983).

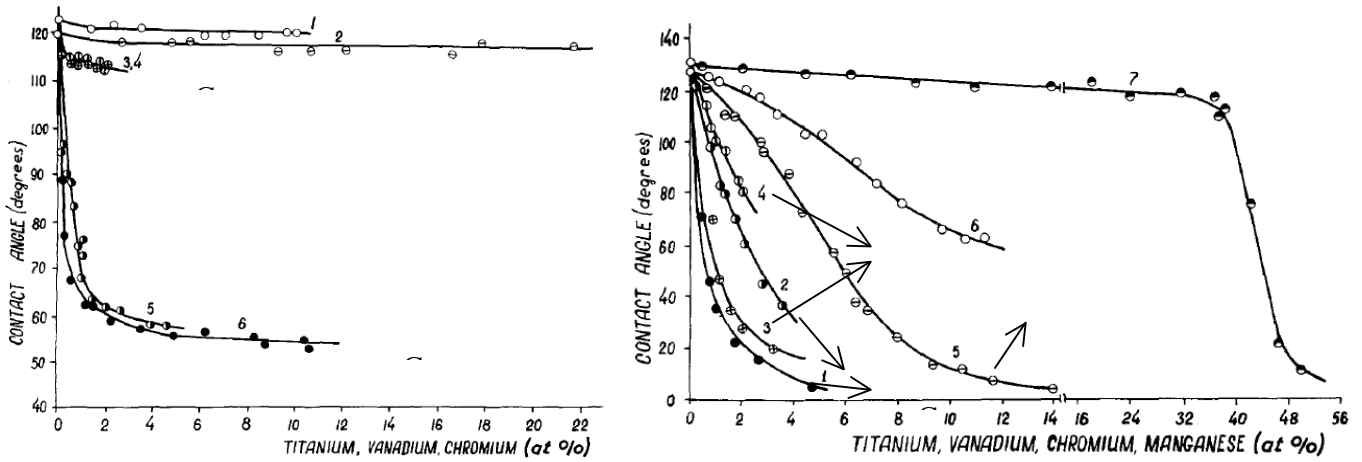


Figure 25. Contact angle of (a) Quartz with Ga-Cr, Ga-V, Ga-Ti, curves 1, 3 and 5 at 900 °C and curves 2, 4 and 6 at 1050 °C (b) Graphite with Ga-Ti, Ga-V, Ga-Cr, Ga-Mn, curves 1, 3 and 5 at 1050 °C and curves 2, 4, 6 and 7 at 900 °C (Naidich and Chuvashov, 1983).

As indicated in Figure 25 (a) and (b), adding 1% (atom) of Ti in Ga at 900 °C, the contact angle between Ga and quartz drops from 120° to 63°, while the contact angle between Ga and graphite drops from 130° to 100°. In Graphite/Ga/Cr system, it was suggested that a transition layer such as CrC_x in Graphite/Ga/Cr system, or TiO , Ti_2O_3 in Quartz/Ga Ti system, and TiC_x in Graphite/Ga/Ti system, is formed at the interface to improve wetting.

The addition of Si in SiC/Ni/Si, SiC/Cu/Si, and SiC/Fe/Si (Liu et al., 2010) improved the wetting because CuSi_2 and NiSi_2 formation in the bulk metal accelerated the spreading kinetics at the interface. Another possible element for improving Ga wetting on SiC might be Mg. As shown in Figure 26, the contact angle of molten Al drops 10° with only 2wt% of Mg addition. Ga and Al are in the same group and share some similar features. Further, Mg may not only improve Ga/SiC wetting, it may also help hydrogen dissociation ability by serving as the M_2 metal.

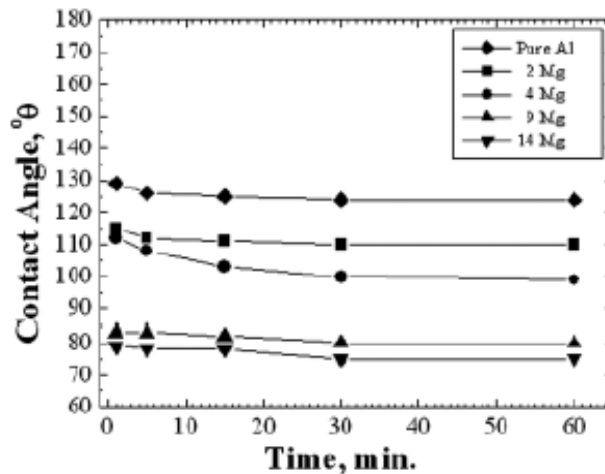


Figure 26. Contact angle of molten Al-Mg on SiC at 750°C [12].

Wetting improvement tests were, thus, performed on coupons. Ga with x -wt% M_2 was pre-annealed in hydrogen environment for 24 hours at 550 °C before depositing on SiC. Then, the coupons were heated under hydrogen for 12 hours at 550 °C. As shown in Figure 27 (a) and (b), the wetting of pure Ga on SiC was moderate at room temperature, possibly due to the trace oxygen adsorption on SiC surface [13] and on molten Ga surface. After heating, however, Ga formed droplet shape on SiC indicating poor wetting.



Figure 27. SiC-Ga wettability coupon tests (a) before (b) after heating.

With 1-wt% M_2 addition as shown in Figure 28 (a) and (b), the distribution of Ga on the surface was scattered and parts of the SiC bare substrate was revealed. The wetting did improve slightly, however, after M_2 addition. However results shown in Figure 29 (b) with 2-wt% M_2 addition followed by heating in hydrogen show that SiC wetting by Ga was substantially better.



Figure 28. SiC-Ga-1wt% M_2 wettability coupon tests (a) before (b) after heating.



Figure 29. SiC-Ga-2wt% M_2 wettability coupon tests (a) before (b) after heating.

7.3 Membrane Support Sandwich Configuration for SMMM

The above results indicate that the wetting can be substantially improved by adding small amounts of appropriate metals M_2 to the molten metal. Further, to ensure that the membrane remains stable even when the gas composition changes, we have developed some designs for SMMM that ensure it by avoiding a free gas-liquid interface, i.e., by sandwiching the membrane between two support layers.

Another key consideration in design of permeators is sealing. There are, in general, three types of possible seals: 1) compressive seal, 2) compliant seal, and 3) rigidly bonded seal. Both compressive and compliant seal involve mechanical compression on ceramic components and gaskets, while rigidly bonded seal, as we have pursued so far, requires careful matching of the thermal coefficient of expansion of the membrane support, substrate, and the sealant glass, to avoid development of leakage during heating and cooling down. Further, the sealant glass has a tendency to react with molten metal. Consequently, we are looking into designs that allow compressive/compliant sealing in a sandwich configuration, while avoiding molten metal contact with any material other than a support which we have found to be relatively inert toward the molten metals. These materials are used for both the porous support layers, as well as for seals and as spacers (washers).

To avoid the change in liquid metal wettability and the resulting change in the supported membrane morphology because of temperature or gas composition changes, thus, one could fabricate a sandwich liquid metal membrane between two support layers, which could, e.g., be porous SiC disks, porous graphite, or perforated vanadium disks, or a combination thereof. The high melting points and high densities of refractory metals such as V preclude penetration and reaction by liquid metals. However, high melting point of the refractory metals also means that fabricating sintered metal tubular supports from these is also difficult or/and expensive. Thus, these metals may be used in perforated form, as shown in Figure 30, which shows a vanadium foil, 1" OD and thickness 0.127 mm, that was laser perforated by us with aperture size 0.010" and space between holes close to 0.030", to serve as a potential support for the liquid metal membrane. This perforated disk was found to be inert toward molten metal in a hydrogen atmosphere for temperatures up to 400 °C.



Figure 30. 1" OD, perforated vanadium foil.

7.4 Swagelok Cell Permeator

The sandwich design is tested in a permeation cell built from Swagelok fittings is shown in Figure 31.

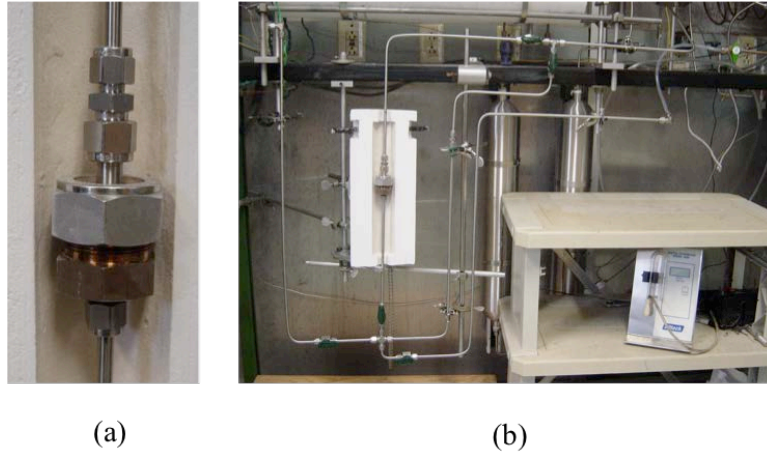


Figure 31. (a) The Swagelok membrane sandwich cell, and (b) its experimental setup.

The key item in this is the specially designed S.S. Swagelok fitting (item 2 Figure 32).

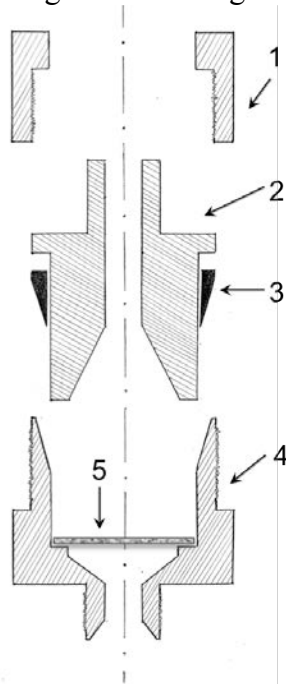


Figure 32. Cross section view of the of cell-permeator assembly for 1"OD metal support for a sandwich SMM membrane. 1 – Swagelok 1"OD stainless steel nut; 2 – stainless steel fitting; 3 – graphite ferrules with 1" ID; 4 - Swagelok stainless steel 1" to 1/4" union; 5 – 1" OD and 0.062" thick porous stainless steel disk.

This fitting provides simultaneous Swagelok sealing of the cell as well as compressive sealing of the membrane support foil/graphite within the cell (Figure 32). The porous stainless steel/SiC disk (item 5 on Figure 32) provides mechanical support for membrane sandwich supported

between two porous layers spaced by a vanadium/carbon paper washer/spacer that determines the membrane thickness and keeps the molten metal from coming in contact with the S.S. housing/porous disk.

8. Conclusions and Future Research

Even though the progress accomplished in this project was less than that planned because of the novelty of the research and an absence of guidance available in the literature to avoid many of the stumbling blocks encountered during the course of this work, on the whole we believe that our original hypothesis has been shown to be sound, namely, that the higher hydrogen diffusion coefficient as well as solubility in molten metals because of lattice defects and vacancies portends the development of non-PGM hydrogen membranes that meet or exceed the DOE targets for 2015. Were opportunity to further develop SMMM to become available, it is clear that work needs to be done to: 1) establish irrefutable potential of SMMM for hydrogen separation, 2) investigate its basic nature, and 3) develop practical designs and investigate their performance under realistic conditions. These are further described below.

8.1 Accomplishments

- ◆ It was found that wettability and chemical inertness are competing requirements. Thus, ceramic supports (e.g., zirconia) possess good inertness but poor wettability, while naked metal supports (e.g., PSS), while readily wetted, react with molten metals at elevated temperatures to form impermeable solid alloys and intermetallic compounds.
- ◆ Coupon studies indicated that PSS oxidized at the usual temperature (700 °C) that works for Pd membranes does not provide an effective diffusion barrier that holds up to the liquid metals tested (In, Ga, Sn).
- ◆ Many ceramic supports are fragile and crack at sealing pressures necessary for effective sealing at higher temperatures. However, promising ceramic support candidates include SiC, ZrO₂, and TiO₂, while others were identified as unsuitable, e.g., quartz.
- ◆ A thermodynamic analysis was performed to theoretically evaluate suitability of different ceramic oxide and nitride supports for wettability and reactivity.
- ◆ SiC was found to be the best ceramic candidate that possesses excellent strength, complete inertness, and adequate wettability to provide dense molten metal membranes.
- ◆ These SiC supported SMM membranes are stable (~250 h) under a hydrogen atmosphere, but when an inert atmosphere is introduced, e.g., He, to check ideal selectivity, the wettability declines because of an increase in liquid-gas surface tension in a He atmosphere.
- ◆ A thermodynamic model was developed that not only explains the change in the liquid-gas surface tension, but also the change in the solid-liquid surface tension and wetting of a molten metal-ceramic system in response to change in the gas-phase composition.
- ◆ It was established that a dense Ga-SiC membrane at 550 °C has a high selectivity and a permeance that is likely higher than that of Pd membranes.

- ◆ The Ga-SiC membrane was also found to thin after extended periods possibly because of volatile hydride formation.
- ◆ A five-step comprehensive microkinetic model was developed for permeation of hydrogen in dense metal membranes, which is suitable for adoption to SMMM when the necessary parameters become available.
- ◆ Based on theoretical and experimental understanding, a novel membrane-support sandwich (MSS) design was developed that may solve the wetting instability issue of SMMM.

8.2 Further Work

- ◆ Utilizing the membrane-support sandwich (MSS) design described above to obtain irrefutable evidence of the SMMM potential and its detailed performance characteristics as a function of temperature and pressure drop.
- ◆ Alloying Ga with small amounts of metals M_2 to improve its wetting.
- ◆ Extending the thermodynamic surface tension and wettability model to understand the effect of H_2/He composition on the wetting characteristics of Ga-SiC membrane.
- ◆ Adapting the theoretical model of hydrogen permeance developed to SMMM and determining the necessary parameters theoretically (DFT) and experimentally, as described below in more detail.
- ◆ Developing the SMMM technology further, by subjecting the SMM membrane developed to rigorous testing of H_2 permeability, selectivity, and durability testing under increasingly realistic conditions of temperature, pressure, gas composition, and poisons.

8.3 SMMM Fundamental Investigation

We also plan, via DFT modeling (Figure 33), to investigate the mechanism and modeling of hydrogen diffusion through molten metal membranes, as well as further thermodynamic analysis of the effect of temperature, gas composition, and the nature of the substrate on wetting of molten metal. We have begun molecular modeling simulations using DFT to model H_2 diffusion and uptake in Ga liquid (Figure 33) using the CP2K software. Long-term goals include evaluating surface adsorption/dissociation of hydrogen, as well as adhesion and wettability of gallium to metal oxide supports. Solubility and diffusivity of H_2 in Ga will also be measured gravimetrically using the tapered element oscillating microbalance TEOM apparatus (Jalani et al., 2005).

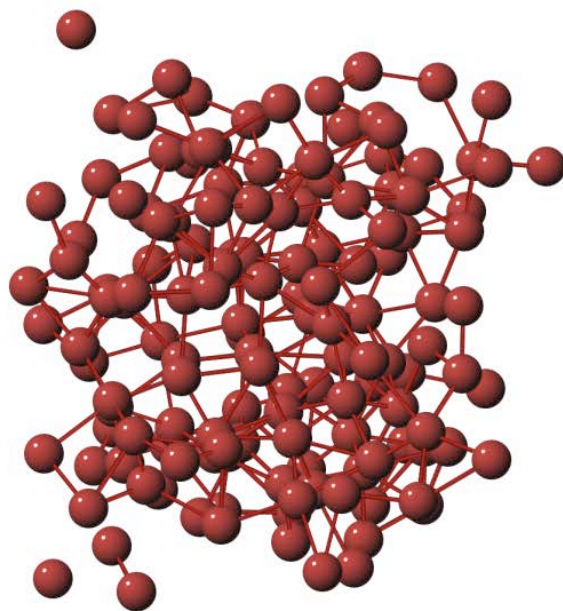


Figure 33. Snapshot of first-principles simulation of liquid Ga.

9. References

- Adhikari, S., and Fernando, S., "Hydrogen Membrane Separation Techniques," *Ind. Eng. Chem. Res.*, **45**, 875-881 (2006).
- Asthana, R. "An Empirical Correlation between Contact Angles and Surface Tension in Some Ceramic-Metal Systems," *Metallurgical and Materials Transactions A*, 25A, (1994), 225-230.
- Ayturk, E. M., Mardilovich, I. P., Engwall, E. E., and Ma, Y. H., "Synthesis of Composite Pd-Porous Stainless Steel (PSS) Membranes with a Pd/Ag Intermetallic Diffusion Barrier," *J. Memb. Sci.*, **285**, 385-394 (2006).
- Candan, E., Atkinson, H. V., Turen, Y., Salaoru, I., Candan, S., "Wettability of Aluminum-Magnesium Alloys on Silicon Carbide Substrates," *Journal of the American Ceramic Society*, 94, 3, 867-874 (2011).
- Chentsov, V. P., Shevchenko, V. G., Mozgovoï, A. G., and Pokrasin, M. A., "Density and surface tension of heavy liquid-metal coolants: Gallium and indium," *Inorganic Materials: Applied Research*, 2(5), 468-473 (2011).
- Cochran, C. N., and Foster, L. M., "Reactions of gallium with quartz and with water vapor, with implications in the synthesis of gallium arsenide," *Journal of The Electrochemical Society*, 109(2), 149-154 (1962).
- Deveau, N.D., Ma, Y.H., and Datta, R., "Beyond Sieverts' Law: A Comprehensive Microkinetic Model of Hydrogen Permeation in Dense Metal Membranes," *J. Memb. Sci.*, **437**, 298-311 (2013).
- do Nascimento, R. M., Martinelli, A. E., Buschelli, A. J. A., "Review Article: Recent Advances in Metal-Ceramic Brazing," *Cerâmica*, 49, 178-198 (2003).
- DOE Report, *Separation Technology R&D Needs for Hydrogen Production in the Chemical and Petrochemical Industries*, (2005).
- Driscoll, D., *NETL Test Protocol – Testing of Hydrogen Separation Membranes*, DOE/NETL – 2008/1335 (2008).
- Elsbergen, V. van, Kampen, T.U., Monch, W., "Surface analysis of 6H-SiC," *Surface Science*, 365, 443-452 (1996).
- Eustathopoulos, N., Nicholas, M. G., Drevet, B., *Wettability at High Temperature*, Pergamon Materials Series 3, Elsevier, (1999).
- Fukai, Y., *The Metal-Hydrogen System*, Springer-Verlag, Berlin (2005).

- Holladay, J.D., J. Hu, D.L. King, Y. Wang, "An overview of hydrogen production technologies," *Catal. Today* 139 (2009) 244–260.
- Iida, T., Guthrie, R. I. L., *The Physical Properties of Liquid Metals*, Clarendon Press, Oxford, (1988).
- Jalani, N. H., Choi, P., and Datta, R., "TEOM: A Novel Technique for Investigating Sorption in Proton-Exchange Membranes," *J. Memb. Sci.*, **254**(1-2), 31-38 (2005).
- Liu, G. W., Muolo, M. L., Valenza, F., Passerone, A.; "Survey on Wetting of SiC by Molten Metals," *Ceramics International*, 36, 1177-1188 (2010).
- Lyon, R. N., Verne Katz, D., *Liquid-Metals Handbook*, United States Office of Naval Research Committee on the Basic Properties of Liquid Metals, Washington U.S. Government Printing, (1950).
- Mazayev, S. N., and Prokofiev, Yu. G., "Hydrogen Inventory in Gallium," *J. Nuc. Materials*, **212-215**, 1497-1498 (1994).
- Naidich, JU. V., Chuvashov, JU. N., "Wettability and Contact Interaction of Gallium-Containing Melts with Non-Metallic Solids," *Journal of Materials Science*, 18, 2071-2080 (1983).
- Nakajima, H., "Fabrication, properties and application of porous metals with directional pores," *Progress in Materials Science*, 52(7), 1091-1173 (2007).
- Nenoff, T.M., R.J. Spontak, C.M. Aberg, "Membranes for hydrogen purification: an important step toward a hydrogen-based economy," *MRS Bull.* 31 (2006) 735–741.
- Ockwig, N. W., and Nenoff, T. M., "Membranes for Hydrogen Separation," *Chem. Rev.*, **107**, 4078-4110 (2007).
- Okamoto, H., "Ag-Ga (Silver-Gallium)," *Journal of Phase Equilibria and Diffusion*, 29(1), 111-111 (2008).
- Paglieri, S.N., J.D. Way, "Innovations in palladium membrane research," *Sep. Purif. Methods* 31 (2002) 1-169.
- Pöttgen, R., "Stannides and Intermetallic Tin Compounds-Fundamentals and Applications," *Zeitschrift für Naturforschung B-Journal of Chemical Sciences*, 61(6), 677-698 (2006).
- Protopapas, P., Andersen, H. C., and Parlee, N. A. D., "Theory of transport in liquid metals. I. Calculation of self-diffusion coefficients," *The Journal of Chemical Physics*, 59, 15 (1973).
- Samsonov, Q. V. "On the Problem of the Classification of Carbides," *Powder Metallurgy and Metal Ceramics*, 4, 1, 75-81 (1965).
- Sholl, D.S., Y.H. Ma, "Dense metal membranes for the production of high purity hydrogen," *MRS Bull.* 31 (2006) 770–773.

- Wert, C., and Zener, C., "Interstitial Atomic Diffusion Coefficients," *Phys. Rev.*, **76**, 1169-1175 (1949).
- Westbrook, J. H., "Intermetallic Compounds: Their Past and Promise," *Metallurgical Transactions A*, **8(9)**, 1327-1360 (1977).
- Yatsenko, S. P., Sabirzyanov, N. A., Yatsenko, A. S., "Dissolution Rates and Solubility of Some Metals in Liquid Gallium and Aluminum," 13th International Conference on Liquid and Amorphous Metals, *Journal of Physics: Conference Series*, **98**, 1-7 (2008).
- Yen, P.-S., and Datta, R., "Butler-Sugimoto Monomolecular Bilayer Interface Model: The Effect of Oxygen on the Surface Tension of a Liquid Metal and its Wetting of a Ceramic," submitted to *J. Colloid & Interf. Sci.* (2014).
- Yun, S., S.T. Oyama, "Correlations in palladium membranes for hydrogen separation: A review," *J. Memb. Sci.*, **375**, 28-45 (2011).